

Msc Thesis

Design validation of the MATE tendon-based passive device for post-stroke rehabilitation

L. Kieft

Msc Thesis

Design validation of the MATE tendon-based passive device for post-stroke rehabilitation

by

L. Kieft

Student Name	Student Number
Levi	4671074

In partial fulfilment of the requirements for the degree of
Master of Science
in Mechanical Engineering
at the Delft University of Technology
to be defended on Thursday October 20, 2022 at 9:00.

Supervisor: Prof. dr. ing. L. Marchal-Crespo,
Supervisor: Prof. dr. ing. H. Vallery,
Project Duration: November, 2021 - October, 2022
Faculty: Faculty of Mechanical, Maritime and Materials Engineering (3mE), Technical University Delft

Thesis Committee: Prof. dr. ing. L. Marchal-Crespo TU Delft
Prof. dr. ing. H. Vallery TU Delft
Dr. ing. J. Kober TU Delft
Dr. ing. J. Moore TU Delft

CONTENTS

I Introduction	3
II MATE Design	4
II-A Working principle	4
II-B Configuration	4
II-C Cable attachment	5
III Experimental Setup	5
III-A Motion capture	5
III-B Lokomat	6
III-C Force Sensors	6
III-D Lokomat trial protocol	7
III-E Human trial protocol	7
III-F Data analysis	7
IV Results	9
IV-A Lokomat	9
IV-B Human	10
V Discussion	13
V-A MATE Design Properties	13
V-B Lokomat	14
V-C Human	14
V-D Limitations	15
V-E Recommendations	15
VI Conclusion	16
References	16
Appendix	18
Appendix A: Force sensors	19
Appendix B: Cable	20
A Diameter Determination	20
B Stiffness	20
Appendix C: MATE	22
A Pulley friction	22
B Attachment	23
Appendix D: Lokomat Joint Space Difference	23
Appendix E: Lokomat Results Expanded	26
A End Effector position	26
B Split Gait	26
C Averaged Gait	27
D Averaged Gait with Phases	28
E Forces	28
Appendix F: Human Results Expanded	30
A Motion Capture Gait	30
B Motion Capture Gait Average	31
C End Effector position	32
D Split Gait	33
E Averaged Gait	34
F Averaged Gait with Phases	35
G Spatio-temporal Correspondence	36
H Forces	38

Appendix G: Force Comparison

Appendix H: Unity

A Motion Tracking

Design validation of the MATE tendon-based passive device for post-stroke rehabilitation

Levi Kieft

Abstract—Rehabilitation robots have been shown to be effective in post-stroke gait rehabilitation. However, these devices are usually expensive and suffer from high inertia which decreases transparency. The Minimally Actuated Tendon-based exercise Environment (MATE) is a tendon-based rehabilitation device, designed to be cost-effective and minimize inertia effects. The MATE must apply minimal forces to the wearer if the gait cycle is healthy to prevent deviation into an unhealthy gait. Previously a mathematical optimization was performed on the design of the MATE. This thesis aims to make a physical realization of the MATE to investigate the minimal forces during a healthy gait cycle with two experiments. The first experiment attached the tendons to a machine to investigate forces on a non-altering gait. HTC VIVE motion trackers were used to measure the position of the tendon attachments over time. To measure the tension, in each cable inline tension sensors were added. Comparing the measured forces to velocity-based thresholds indicates that the forces applied by the MATE are too high and would cause deviation. The second experiment involved a human walking with and without the MATE. Evaluating the gait cycle trajectory when walking with and without the MATE indicates that the MATE alters a healthy gait cycle, lowering the step height and causing drift. The forces acting on this gait also exceed the thresholds. The MATE in its current design alters a healthy gait. Redesigning the MATE with the suggestions from this thesis will likely show further improvements.

Index Terms: end-effector, gait, rehabilitation, therapy, stroke

I. INTRODUCTION

When investigating the leading causes of death and disabilities in the world with the disability-adjusted life-years lost metric, stroke remains third [1], with 12.2 million occurrences of stroke leading to 6.55 million deaths in 2019 and a total amount of strokes that persisted of 143 million, this is an increase of 70% in incidence (occurrence) and 85% in prevalence (persisting) since 1990 [2]. The effects of stroke generally affect one side of the body, resulting in hemiparesis [3]. Post-stroke, around 80% of the survivors suffer from a loss in mobility or muscle control [4] [5], which can affect gait pattern functions and possibly result in the loss of independent walking ability [6]. Even for those who learn to walk independently again, the persisting condition impacts the quality of their life [7].

The amount of people who are in need of rehabilitation due to stroke increases each year [1]. One of the main goals of rehabilitation is the recovery of independence through walking [8]. Most recovery occurs within the first three months after stroke [6], thus patients should start rehabilitation as soon as possible. A common method of rehabilitation is bodyweight supported treadmill training. During this one or more physiotherapists guide the walking cycle of the patient

using a treadmill and a body weight support system (BWS) [9]. This can overexert the therapists and is a limiting factor in rehabilitation [10]. Using robotic devices with physiotherapy increases likelihood of better results [6], increasing the length and amount of sessions [9]. Furthermore, robotic assistance relieves stress from the therapist [11] and can be preferable to human assistance [10].

An investigation into the most prominent lower-limb rehabilitation classifies two groups of stationary systems, those that use a treadmill and those that have programmable foot end-effectors [9]. Treadmill-based devices commonly use an exoskeleton in accordance with a BWS to provide forces to the joints of the leg, whilst the end-effector approach only guides the feet and leaves the hips and other joints free [9] [6]. These devices are not without issues [12], such as high cost and limited transparency. Tendon-based alternatives are being developed, both to the exoskeleton [13] and to end-effector approach [14] in order to improve load, speed, adjustable stiffness and personalization. Implementing cable-driven robots for gait rehabilitation has been previously proven to be effective [15] [16] [17].

An issue that these alternatives do not account for is about the cost of these devices [18]. The devices are complex and cannot easily penetrate the market, leading to a high cost of research but low amounts of sales, which drives up the cost of the devices, varying from \$9,000 up to \$100,000 [19]. Due to this cost only 5% to 15% of the people who need them have access to these devices [18]. Especially in lower and lower-middle income countries, where around 90% of the burden of stroke lies [1], the cost is a large factor in why they cannot have access to these devices.

The Minimally Actuated Tendon-based exercise Environment (MATE) was designed [20] with the aim to produce a transparent and affordable rehabilitation robot. Using the fact that most patients are hemiparetic [3], the concept uses the force of the non-paretic leg to drive the movement of the paretic leg. It resembles the tendon-based device of [14] but removes all actuators and instead connects the tendons between the legs. These tendons will be passive, with no actuators. This design has not been developed or tested, therefore the effectiveness of generating a physiological gait or the production of any unwanted, parasitic forces is unknown. This report aims to build the MATE and test it. First with a robot-driven physiological gait where the parasitic forces are measured. Then with human-driven pathological gait, evaluating the effectiveness of guiding the human back to a physiological gait cycle.

In order to achieve this, the initial design from [20] is finalized and realized. Then, a Lokomat rehabilitation device (Hocoma, Switzerland) is used to generate a physiological gait.

The tendon forces are measured and evaluated against thresholds that alter the gait [21]. Additionally, human participants will recreate pathological gait cycles both with and without wearing the MATE. Using motion tracking, the gait cycles are compared to see if the MATE brings a pathological gait to a physiological gait. A survey will answer questions about the comfort and perceived effect of the device.

II. MATE DESIGN

The design of the MATE as from [20] has been further developed in order to create a testable device. The principle behind the design, what properties that brings along and the configuration used for the final build are expanded below.

A. Working principle

The MATE as it was built can be seen in [Figure 1](#). The device is built around the treadmill of a Lokomat, anchored to the frame of the Lokomat with bolts through the original holes. The MATE frame is 1.8 m long, 1.0 m wide and 1.2 m high. The Lokomat expands these dimensions. The frame is made from aluminium profiles that were available in-house.

The Lokomat is controlled by an external computer. That computer communicates with xPc target computers to the actuators (LokoFree) and to the BWS and treadmill (LokoBase). The Lokomat is controlled with a compliance control or PD-controller. The gains have been tuned by a local PHD'er to replicate high stiffness. As the Lokomat is a custom configuration modified by [22] these gains do not generalize to other Lokomat devices. They are also dependent on the frequency. For these reasons the gains are not specified, the Lokomat is assumed to act with high stiffness. A validation of this will be performed in the joint space difference in [section D](#). More details on the electrical scheme of the Lokomat can be found in [31] and about the modifications in [22].

The BWS as originally part of the Lokomat has been modified to be able to move sideways. This movement allows that the weight compensation force is applied vertically even if the participant drifts sideways. The details of this modification can be found in [22]. Due to the modifications, the amount of BWS weight compensation has to be set manually. It can be set in any range from no support to fully lifting the person. The maximum support allows for the full lift of a person of up to at least 80 kg. Separately from the weight compensation, there is a safety measure that limits the maximum length of the BWS support cable. This ensures that if a person wearing the BWS trips they do not hit their knees on the floor, instead becoming fully suspended into the air (up to the maximum weight).

The MATE connects four elastic cables to each leg to control the three (3) translational (x-, y- and z-position) Degrees of Freedom (DoF). A Matlab visualisation of the MATE attached to a person with axes definitions can be seen in [Figure 2](#). Since the cables can only apply tension forces, one more cable than DoF is needed [23], so the MATE uses four (4) cables to control three (3) DoF. To further minimize inertia and cost, these cables are attached to a single cuff around the shin. These cables are attached between the legs, for example the

front upper cable of the left leg is the same cable as the front upper cable of the right leg. The force that each cable applies to the legs is determined by the elongation of the cable and its stiffness. The elongation is determined by the gait pattern and cannot be predetermined. The stiffness of each cable is derived from the desired horizontal stiffness. The applied force acts in different directions based on the placement of the pulleys on the frame. To keep the cables on the pulleys during the full gait cycle, the pulleys need to be able to rotate such that the cable and pulley are always properly aligned, for this reason single revolute joint pulleys were implemented.

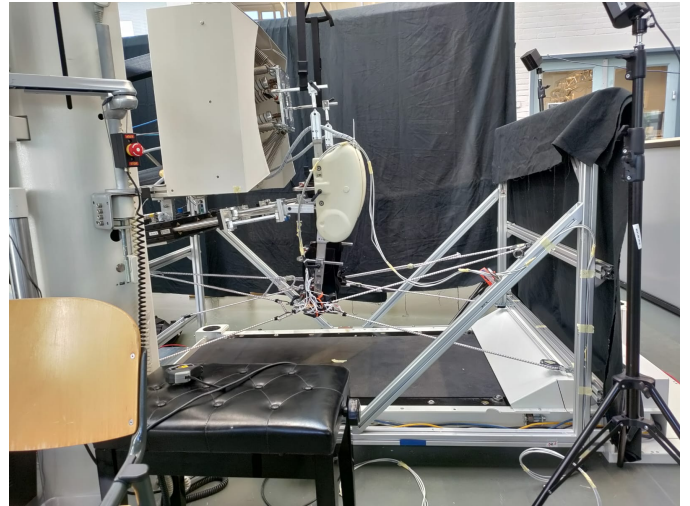


Fig. 1. MATE attached to the Lokomat

B. Configuration

The design of the MATE is based around the positioning of the tendons. The position and placement of the pulleys can be seen in [Figure 2](#). The purpose of the MATE is a device that can apply forces to the lower limbs in order to assist the user with reaching a physiological gait. To realise the optimal cable placement from [20] and to allow for experimentation, additional development took place. There are six (6) pulleys used in the MATE. Three (3) of these are on the front frame, the other three (3) are on the back. Two (2) pulleys will be placed higher, named pulley 'fh' in front and pulley 'bh' in the back, meaning 'front high' and 'back high' respectively. Four (4) pulleys will be placed lower, named 'fl_l', 'fl_r', 'bl_r' and 'bl_l' meaning 'front low left', 'front low right', 'back low left' and 'back low right' respectively. It is assumed during calculations that these pulleys have negligible friction, a validation is performed in [subsection A](#).

In order to ensure physiological gait, the design minimizes the forces that the device produces during a physiological gait with the horizontal stiffness was set at 1 kN/m based on other lower-limb rehabilitation devices [24] [25]. To achieve this, they minimized the sum of the root mean squared error (RMSE) of the parasitic cable forces in all Cartesian directions for both legs over physiological gaits. This optimization was previously performed [20] and resulted in the optimal pulley

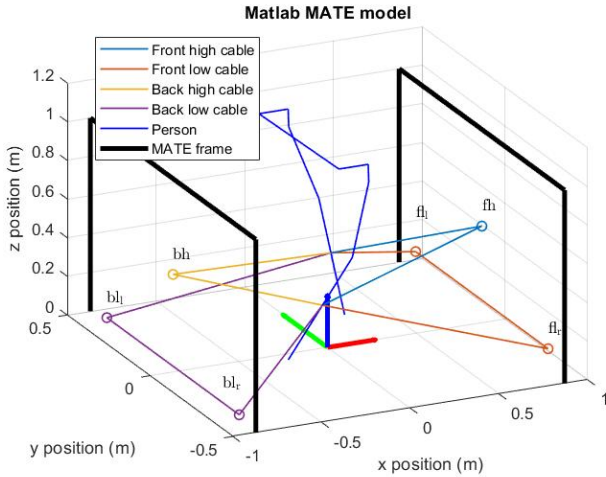


Fig. 2. Matlab MATE visualisation with the four (4) cables attached to a skeleton with axes and pulley name definitions.

placements of [Table 1](#). This optimization did not account for the boundaries of the Lokomat. This affects the z_{bh} value, as the highest possible value without colliding with the Lokomat is 0.5 m. Similarly, the position of the front and back pulleys in the x-axis was set to be 0.75 m, but due to the constraints on the design of the frame this distance in the realised MATE was 0.895 m. The pulley placements in the built MATE approach these values as close as they can, see the 'implemented' row in [Table 1](#).

Transposing the horizontal stiffness of 1 kN/m to the cable tension using Jacobians gives a stiffness of 300 N/m for the cables [\[20\]](#). This stiffness can be achieved by either connecting a series elastic element [\[26\]](#) [\[27\]](#) or by using an elastic cable. No similar applications that make use of an elastic cable have been found. Still it offers advantages and counters reasons that would make implementing an SEA difficult. An elastic element is not able to move over a pulley. As both ends of the cable are connected to the legs, the position of the elastic element moves and could be too close to a pulley, depending on the range of motion. However, replacing the SEA with an elastic cable removes the ability to put a sensor on the SEA that can accurately measure the elongation and thus the forces. This can be mended by implementing inline tension sensors.

Building on the Matlab simulation used by [\[20\]](#), additions were made to investigate the expected elongation of the cables. This resulted in 7% elongation depending on the cable, setup and participant, see [subsection II-C](#). Bungee cables can elongate up to twice their length [\[28\]](#), but keeping the maximum elongation below 30% is recommended. A calculation, more details in [section B](#) shows that an 8 mm cable has the 300 N/m stiffness required. A validation of this stiffness has been performed, see [subsection B](#) that shows that the actual stiffness is only around 160 N/m.

By investigating the minimum length of a cable in simulation and accounting for any components in the built MATE that add to this length, such as the attachments, the minimum length of the cable is determined. This length can be varied

by changing the attachment, so the pretension can be set independent of this length. The pretension is set by tightening the elastic cables whilst the participant or Lokomat is in a neutral position.

C. Cable attachment

The cables are attached to the tracker straps. These are Velcro straps made to fit the HTC VIVE trackers. On the side of these straps are hard plastic loops. The cables are attached with cable hooks to these loops. These attachments are not rigid and a design for new attachments has been made, see [subsection B](#).

III. EXPERIMENTAL SETUP

In order to validate the design of the MATE, experiments were performed with the Lokomat replaying a generated gait and a human participant. The Lokomat experiment is used to investigate the magnitude and direction of the cable forces. The magnitude is measured using the inline tension sensors and using motion capture and forward kinematics the gait trajectories can be determined. The goal for the experiments with a person is to determine the difference between their gait with and without the MATE. This is done by using motion capture in both scenarios. Then the participant is asked to purposefully deviate from their normal gait and experience whether the MATE acts to realign them.

A. Motion capture

Motion capture is used to determine the coordinates of the shins where the cables are attached. From the recorded cable attachment coordinates gait cycles can be visualised and compared. To this end, a HTC Vive Pro 2 (HTC Corporation, Taiwan) system is used combined with SteamVR (Valve Corporation, USA) software. The used components were a headset, two trackers and two lighthouses. The lighthouses are used to create the field of view. Only objects within the view of the lighthouses can be tracked. Each lighthouse sends out infrared (IR) light flash. The trackers and headset send a signal to the computer to start counting once they get hit by IR. Then, the lighthouse sends out a tracker IR laser in vertical and horizontal directions. When a tracker or headset gets hit by this laser they send a signal to stop the counter. From the value of this counter, the computer running SteamVR determines the 3d pose of the tracked object.

The lighthouses are placed approximately 2 meters in front of the center of the treadmill and 1 meter to either side. Due to the auto calibration feature of the device no exact placements are needed. The head mounted display is placed on a table to the side with full vision of the treadmill. The trackers are placed at the point of attachment of the cables on both legs (Lokomat or human) using a Velcro strap, facing forwards. The strap has been designed so that the tracker can be easily attached and detached without removing the strap.

The tracking happens at about 60 Hz [\[29\]](#). Using two (2) lighthouses, the mean absolute position error is expected to be around 3.5 mm and a standard deviation of less than 1 mm

TABLE I
PULLEY CONFIGURATION, OPTIMAL FROM [20] AND THE IMPLEMENTED VALUES IN THE BUILT MATE

parameters	x_{fh}	z_{fh}	x_{fl}	z_{fl}	x_{fr}	z_{fr}	x_{bh}	z_{bh}	x_{bl}	z_{bl}	x_{br}	z_{br}
optimal	0.00 m	0.50 m	0.40 m	0.10 m	-0.40 m	0.10 m	0.00 m	0.80 m	-0.40 m	0.10 m	0.40 m	0.10 m
implemented	0.00 m	0.50 m	0.40 m	0.13 m	-0.40 m	0.13 m	0.00 m	0.50 m	-0.40 m	0.10 m	0.40 m	0.10 m

TABLE II
LENGTH RANGE OF THE CABLES, OPTIMAL PARAMETERS 1

	subject	tendon			
		tfu	tfl	tru	trl
minimum length (m)	subject 1	1.9223	1.8371	2.3203	1.8371
	subject 2	1.9672	1.8840	2.3576	1.8840
	subject 3	1.9603	1.8769	2.3519	1.8769
	subject 4	1.9478	1.8638	2.3415	1.8638
	subject 5	1.9591	1.8756	2.3510	1.8756
	subject 6	1.9345	1.8499	2.3304	1.8499
maximum length (m)	subject 1	1.9548	1.8711	2.3474	1.8711
	subject 2	1.9921	1.9100	2.3784	1.9100
	subject 3	1.9971	1.9153	2.3827	1.9153
	subject 4	1.9846	1.9022	2.3721	1.9022
	subject 5	1.9855	1.9032	2.3729	1.9032
	subject 6	1.9545	1.8707	2.3470	1.8707
overall minimum	- (1)	1.9223	1.8371	2.3203	1.8371
overall maximum	- (3)	1.9971	1.9153	2.3827	1.9153
difference	-	0.0748	0.0782	0.0624	0.0782

[30], with the major impacts on this error due to systematic effects, such as a tilted plate estimate. The recording of the Unity data occurs at approximately 500 Hz as seen in subsection A.

A calibration is proposed to account for these systematic errors. A set of known coordinates is prepared in the frame of the Lokomat, a square of known dimensions is made on a planar surface. After the Lighthouses are turned on, initial calibration is performed with the headset using SteamVR. For this, the headset is placed on the floor approximating the middle of the treadmill. The headset is then set aside and this square is placed. A tracker is located to each corner of this square and placed there for up to five (5) seconds. A separate manually-controlled variable is used to store which corner the tracker is on during calibration, or whether the tracker is not on a corner. The measured corner positions in the VR coordinate system are compared to the defined corner positions in the global coordinate system, see Figure 2. A transformation is determined between these sets of points. This transformation is used to align the collected data with the global coordinate system. More details about this calibration can be found in subsection A.

Using Unity (Unity Technologies, USA) and a SteamVR plugin, the data of these trackers can be recorded. The calibration data is visualised in Matlab to check for any large deficiencies, such as the connection with a tracker being lost. This tests communication and storage of the data.

B. Lokomat

With the calibration and setup of the motion capture performed, the Lokomat setup follows. The Lokomat is controlled by an external computer with all the motor drivers that communicate with a local computer through ethercad as an xPc target with Matlab Simulink models. A command is send

to the treadmill to see whether it accelerates properly and communication is stable. The BWS is set to different heights and strengths to check for any defects.

If no human participates, the Lokomat motors are placed above the treadmill and fixed. The BWS is attached to the Lokomat, simulating the support the Lokomat would get from a human. This connection lifts the Lokomat plate until the four springs attached to the plate are horizontal. The code for running the gait cycle is tested to see if all communication is functional. The Lokomat is brought back to a neutral resting position and turned off for the remainder of the setup, so that there are no powered motors when a person needs to interact with the device.

When using the Lokomat motors, the data of the motor positions is stored. The positions of the two (2) linear actuators for each leg, one (1) linear actuator of the pelvis and the two (2) knee angles are stored, in addition to the pose of the pelvis plate. This data is retrieved from the xPc log.

C. Force Sensors

The force sensors are used to measure the tension in the cables. Two Scaime CPJ analog transmitters (Scaime, France) are used to amplify the signals so that the sensors give out a value between -10 and 10 volts. This voltage linearly increases with the weight put on the sensor, going from 0 V to 10 V at a weight of 0 kg and 30 kg respectively. The signals are send to a NyDAQ USB-6001 (National Instruments, USA) which connects to the main computer, which can read the values using LabView. This happens at about 20 Hz, which was set by the designer of the sensors. Later testing revealed that the frequency can be increased to at least 200 Hz without errors, see section A. Using Transmission Control Protocol (TCP), the values are loaded into Unity to synchronise with the motion capture data.

These sensors have been tested for their linearity, each has a slightly different slope which is stored and used to convert the voltage information to newtons, but each slope was determined linear using linear regression with an R^2 value of above 0.99. A weight of 5 kg was suspended on one of the sensors for an hour to see if the measured value changed. The measurements shifted indicating bias, so before and after each run of the experiment the force sensor values will be saved with 0 kg suspension. The difference between these values is assumed to have been changing linearly over the time non-zero forces are applied to the sensors. By linearly changing from the pre-experiment bias to the post-experiment bias the actual bias is minimized. More information and the results of these experiments can be found in A.

These force sensors are attached on one side to the elastic cables with a hook. On the other side they are attached to a band around the right leg. The wires from each sensor are

routed up via the leg and then cross over to the MATE frame at hip heights. This keeps the wires out of the way of the legs.

D. Lokomat trial protocol

The setup for the motion control, Lokomat and force sensors are performed. One person will be present on site, dedicated to monitoring the experiment and data collection, hence referred to as the monitor. The monitor will also have access to an emergency stop that can drop power from all the actuators.

Within this experiment, no human participants are included. The single “participant” is the Lokomat device. It has no gender and has been at the TU for about a year.

The MATE is attached to the Lokomat. The Lokomat runs for ten (10) gait cycles following a predefined gait cycle, to allow for a brief transition at the start and end. The Lokomat is then stopped and turned off.

E. Human trial protocol

Ethical approval by the TU Delft Human Research Ethics Committee was received prior to these experiments, including safety reports and data protection. The setup of the motion capture, treadmill, BWS and force sensors are performed before the participant arrives. When they arrive, two other people will be present on-site. One will be dedicated to monitoring the experiment and data collection, hence referred to as the monitor. The other will assist the participant and be ready to hit the emergency stop, henceforth referred to as the surveyor.

There was one (1) participant in this experiment. This participant was 1.76 m tall.

As the participant arrives, the experiment will be explained to them and they have the time to ask questions. They can ask questions at any point during the experiment, as well as revoke their participation at no cost or risk to them. Then they will be helped into the BWS system. They will put on a harness and that is attached to the BWS system at four corners. The BWS is then calibrated to the height of this person, it is used to prevent tripping and falling but is not set to lift part of the bodyweight. Once they are on the treadmill in the BWS, the motion capture trackers are placed around their shins. The monitor confirms that the trackers are seen by the system.

The participant is given some time, up to a minute, to adjust to the BWS and the range of motion. If the participant is prepared, they will be notified that the treadmill will start to move. The treadmill is gradually accelerated to 2.25 km/h. The monitor adjusts this speed at the request of the participant to make the speed feel most natural to them. Once this speed is determined, the participant is asked to walk for three (3) minutes, which is a high time estimate for a hundred (100) steps with each leg including transition time. The participant is notified and the treadmill slows to a halt. Depending on the comfort of the participant, they may be detached and sit or continue straight to the second part of the experiment.

Once the participant is comfortable with moving on, they will be placed back on the treadmill with the BWS attached. Additional to the trackers, the MATE and force sensors are attached. The monitor validates that the force sensors can

be read. The participant is given up to two (2) minutes to acclimate to moving with the assistance of the MATE. Once they feel ready, they are notified and the treadmill is brought to the same speed as determined in the first round. They will walk for three (3) minutes to measure the same hundred (100) steps. The participant is notified and the treadmill is brought to a halt. The MATE is detached and the BWS is lowered, the trackers are removed.

The participant is able to sit and rest if desired. Once they are ready, the third part of the experiment commences. The same setup as for the second part is used, excluding the motion capture trackers. The participants are notified and the treadmill starts moving at their desired speed. The participants are asked to deviate from their normal gait by increasing and decreasing their stride. After three (3) minutes where they fake different pathological gaits they are notified and the treadmill slows to a halt. The MATE is detached, the BWS lowered and the suit is removed.

Since this is not their normal gait, they will not be able to perfectly reproduce the gait with and without the MATE and thus no comparison is made. After the three (3) rounds of walking, the participant is asked to take a seat and talk about their comfort and their experience using the MATE with a fake pathological gait.

F. Data analysis

The experiments differ in what data they collect, though there is overlap. Both experiments gather 3d pose data from the VR trackers and the force sensor data. This information is stored in an .csv (Excel) document. It contains the Unity system time and the poses of the left and right trackers. The axes of the Unity frame are defined differently from the global frame as defined in [Figure 2](#). The unity x-axis is opposite the global y-axis, Unity y-axis is the global z-axis and the Unity z-axis is the global x-axis. The transformation determined from the Unity calibration performed before the experiments is then used to transform the motion capture data with the global frame. Additionally the force sensor data is stored. This data is recorded with Unity system time from the TCP communication with LabView.

A ‘Walking’ variable is used to synch the data between the Lokomat output and the Unity output. As the Lokomat starts its walking cycle, a digital output is changed from 0 to 1. This is measured by the NyDAQ. As long as the Lokomat is walking, this variable is 1, otherwise it is 0. Using this, the recorded data from the Lokomat xPc and the Unity recording can be synched, as both recordings have an interval where this value is 1. This fact is also used to downsample the faster recording so that the frequency matches between the recordings. This is needed for calculation purposes as the matrices need to be of identical length for most calculations. The Lokomat outputs its data as a Matlab double. The double contains the xyz position and rotation of the pelvis plate, the positions of the five (5) linear actuators and the two (2) knee angles. The ‘Walking’ variable is also recorded.

During the experiment with human participants, the monitor will set the ‘Walking’ variable to 1 manually once the treadmill

runs at a speed comfortable to the participant. This makes differentiating the data between transitioning phases and the constant walking phase easier to detect. Similarly, this value is set to 0 before the treadmill is slowed to a halt. Additional to the machine data, the human participants can leave comments to indicate their experience with the MATE and leave feedback.

These experiments function as a validation of the design of the MATE. No large scale experimentation is performed, therefore there is only a small amount of data. This data will form an indication of the working of the MATE.

The motion capture data is synchronised with the Lokomat output using the ‘Walking’ variable. Where this variable is ‘1’, the Lokomat is walking. The two sets of data are sampled to have the same amount of points while this variable is ‘1’. The motion capture data is transformed to the global coordinate system with the transformation matrix determined by calibration. The Lokomat data is changed into attachment point coordinates by using the forward kinematics as defined in [31]. The walking data is split between completed gait cycles using the point of heel strike of the left leg as the start and end of a cycle. The maximum x value closely corresponds to the heel strike. The attachment point positions of both forward kinematics and motion capture are averaged over these gait cycles. Then the motion capture data and forward kinematics can be combined by:

$$Pos_{tot} = p * Pos_{fk} + (1 - p) * Pos_{mc} \quad (1)$$

Where Pos_{tot} is the averaged position of the attachment point, p is the weight factor between the averages. Pos_{fk} is the attachment point position resulting from the forward kinematics and Pos_{mc} the position resulting from the transformed motion capture data. For the purpose of comparing between the Lokomat and human results, p is set to 0 such that only the motion capture data is used for further calculations.

The force sensor data of the Lokomat experiment is stored together with the motion capture data. Using the same data split to determine individual gait cycles, the force is averaged over the gait cycle. Then the force is decomposed into Cartesian directions and summed. This sum is compared to a velocity based threshold. In order to compare the results with the Matlab simulation of [20], the same thresholds are used. These thresholds are a direct function of a constant multiplied with the shin velocity, defined as:

$$T_x = A_x \times v_x \quad (2)$$

$$T_z = A_z \times v_x \quad (3)$$

where T_x and T_z are the thresholds for the forces. A_x and A_z are constants that determine the magnitude of the threshold as determined in [21]. v_x is the forward velocity of the attachment point. As the forces act on the shin instead of on the foot as in [21], both the forces and velocity are chosen on the attachment point. These thresholds must be multiplied by the weight of the person walking to get the actual force thresholds, or the measured forces must be divided by the

weight. Here the forces shall be divided by the weight as was done in [20].

As the effect of a force depends on what part of the gait cycle the attachment point is in, several phases are defined, simplified from [32]. These phases will be defined for a walking gait, not a running gait, so there will be phases where both legs are touching the ground. For a visualisation of the phases, see Figure 3. There are two main phases, ‘Stance’ (60% of the total duration) and ‘Swing’ (40% of the total duration). ‘Stance’ is further divided into ‘Initial Double Support’ (10% of the total duration), ‘Single Support’ (40% of the total duration) and ‘Terminal Double Support’ (10% of the total duration) [32]. The definitions of the phases will be given for the left leg. ‘Swing’ is defined as the period from left leg toe-off to left leg heel-strike. ‘Initial Double Support’ is the period from left leg heel-strike to right leg toe-off. ‘Single Support’ is the period between right leg toe-off and right leg heel-strike, which is the ‘Swing’ period of the right leg. ‘Terminal Double Support’ is from right leg heel-strike to left leg toe-off. Heel-strike and toe-off moments will be approximated by taking the minimum and maximum x-value of a gait cycle, where the maximum is a heel-strike and the minimum is toe-off. These phases will be visualised in the force graphs, but no other metrics depend on the phase.

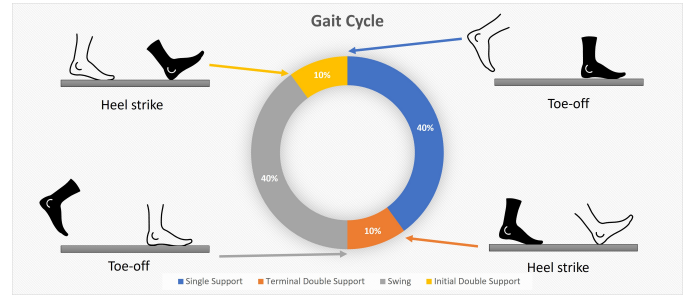


Fig. 3. The four phases of a gait cycle, ‘Initial Double Support’, ‘Single Support’, ‘Terminal Double Support’ and ‘Swing’

The motion capture data collected during the human experiment is compared between walking a gait with and without the MATE, the first two parts of the experiment. Using the ‘Walking’ variable, the walking periods with and without the MATE periods are extracted. The same length of time is used for the calculations with both periods. The length of the two walking periods was made equal by cutting off part of the longer period. As the data is recorded with the same frequency, this corresponds to the same amount of time. These gait datasets are transformed to the global coordinate system using the transformation from the motion capture calibration. Then the datasets are reduced to a gait average by splitting the data into independent gait cycles. To synch the gaits, the peaks of the x-position data are determined. As the x-axis is aligned with the step direction, it has the largest deviation and the clearest peaks. Between these peaks is a single step. These steps are interpolated to be a thousand (1000) datapoints. These individual cycles are averaged over gait cycle percentage.

The mean gait cycles with and without the MATE are spatiotemporally compared, investigating both the difference in 3D position but also the differences in speed. There are no metrics implemented to do this comparison. The mean gait cycles will be visualised and lines drawn between every percent of the gait cycle.

The collected force sensor data of the human experiment is decomposed into Cartesian directions using the motion capture estimate of the attachment points combined with the known MATE pulley configuration. Using the heel strikes as a start, this data is plotted against the percentage of the gait, so that at each point the forces acting on the legs are known. This is compared to the same threshold as above.

The comments of the participant are used as an indication of the MATE experience and functionality. The comments will be taken into account in the discussion and can possibly explain certain errors in the experiment.

IV. RESULTS

A. Lokomat

For these results only single images and for the left leg are shown, for more images see [section E](#). The forward kinematics of the Lokomat were combined with the motion capture data to determine the tracker positions. The forward kinematics and motion capture data were combined to determine the left and right cable attachment coordinates, for the left leg resulting in [Figure 4](#). Splitting the gait data, see [Figure 5](#), for each step and averaging the steps over gait cycle results in attachment positions as seen in [Figure 6](#). The force sensor values can be seen in [Figure 7](#), the walking range is extracted [Figure 8](#). The force sensors averaged over gait cycle percentage can be seen in [Figure 9](#). Sensor 1 was faulty, so the experiment was repeated 4 (four) times. Each repetition had a different sensor replaced with the faulty one. These four measurements were averaged to have an estimation of the forces, resulting in [Figure 10](#).

Determining the difference between the cable attachments and the pulley placements gives the direction of the cables. With this the force vectors are decomposed into their Cartesian directions and summed, see [Figure 11](#). The sum forces compared to the threshold can be seen in [Figure 12](#).

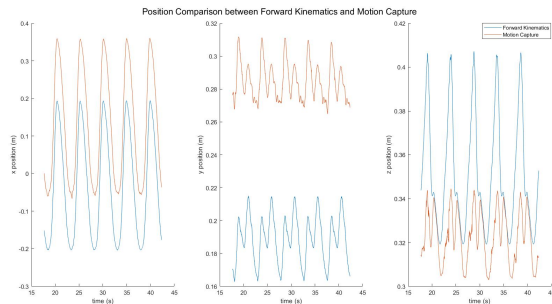


Fig. 4. Attachment point coordinates of the left leg from the forward kinematics and motion capture data, with MATE

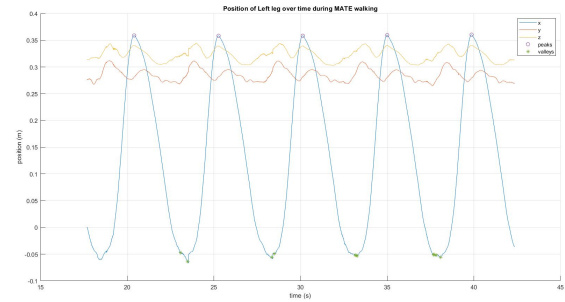


Fig. 5. Cartesian positions of the left leg motion tracker during the duration of walking with MATE

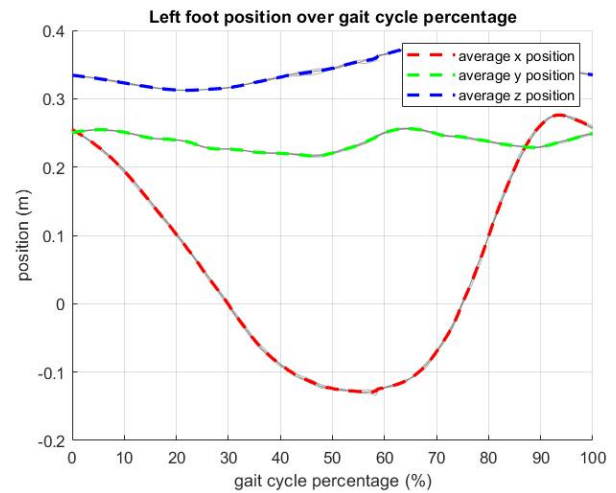


Fig. 6. Attachment point coordinates of the left leg averaged over the gait cycle

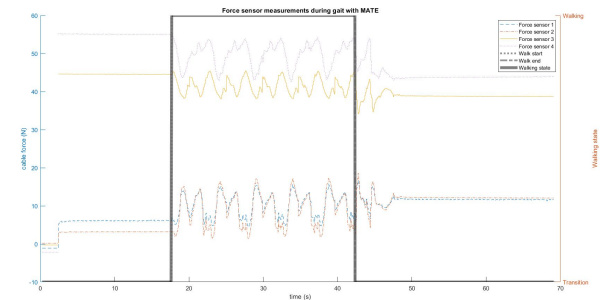


Fig. 7. Forces acting in the cables over the full measured time, with additionally the 'Walking' variable depicted

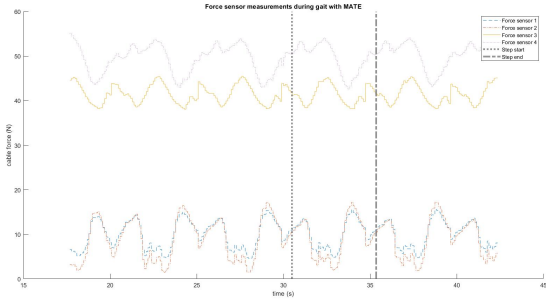


Fig. 8. Forces acting in the cables over the walking period, a single step outlined

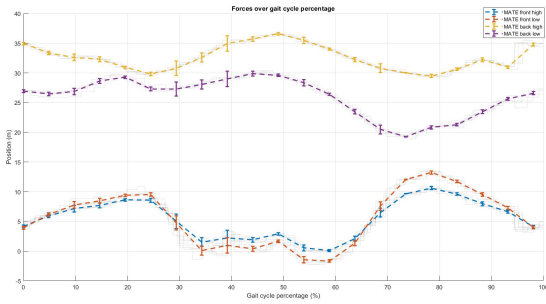


Fig. 9. Forces acting in the cables averaged over the gait cycle

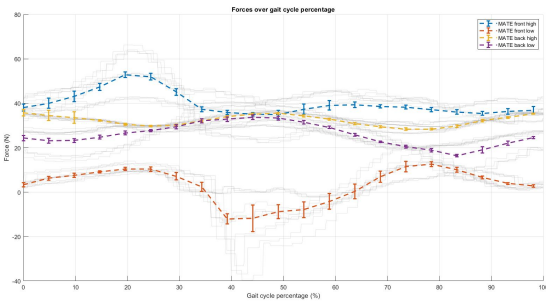


Fig. 10. Forces acting in the cables averaged over the gait cycle, averaged over 4 trials

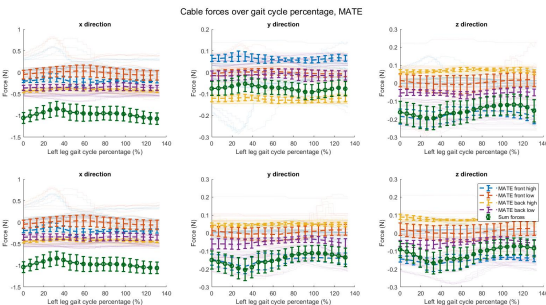


Fig. 11. Forces decomposed into Cartesian x-z axes, summed

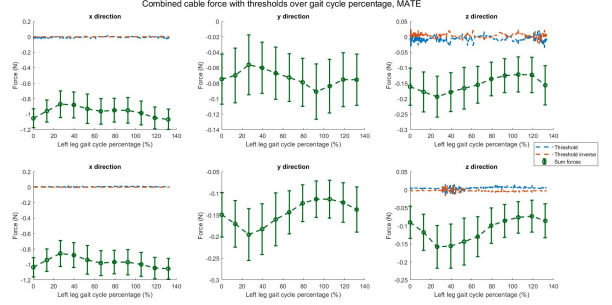


Fig. 12. Forces summed in Cartesian x-z axes compared to threshold forces as determined by [21]

B. Human

The experiments with a human participant in the MATE has results for each leg individually and comparisons between situations. To keep the amount of figures to a minimum, the left leg during free walking figures are presented here. The figures for all the legs can be found in [6]. First, the similarities between the motion capture data of the gaits with and without the MATE are shown. To this end, the motion capture data is transformed with the performed motion capture calibration, resulting in [Figure 13]. The pre and post calibration matrices can be found in [Table III] and [Table IV] respectively. The experiment calibration results are expanded in [subsection A]. The visualisation of the 3D motion capture coordinates of [Figure 13] is averaged to a single gait seen in [Figure 14]. For a single leg seen from 3 sides, see [Figure 15] and [Figure 16]. This average was made by splitting the recorded gait trajectory at the peaks from the x position as seen in [Figure 17]. Extracting the gaits [Figure 18] and averaging them over the gait cycle percentage results in [Figure 19]. Additionally, in [Figure 20] the gait phases of the leg are shown. Visualisations of the spatio-temporal correlation between walking free or with the MATE in all Cartesian directions can be seen in [Figure 21]. The gait patterns are analysed and gait properties are extracted, see [Figure IV-B].

TABLE III
TRANSFORMATION MATRIX PRE-EXPERIMENT MOTION CAPTURE CALIBRATION

$$A_{\text{pre}} = \begin{bmatrix} 0.915 & -0.402 & -0.016 & -0.359 \\ 0.402 & 0.916 & 0.003 & 0.054 \\ 0.013 & -0.009 & 1.000 & -0.180 \\ 0 & 0 & 0 & 1 \end{bmatrix}$$

TABLE IV
TRANSFORMATION MATRIX POST-EXPERIMENT MOTION CAPTURE CALIBRATION

$$A_{\text{post}} = \begin{bmatrix} 0.908 & -0.419 & -0.028 & -0.381 \\ 0.419 & 0.908 & 0.006 & 0.021 \\ 0.023 & -0.017 & 1.000 & -0.109 \\ 0 & 0 & 0 & 1 \end{bmatrix}$$

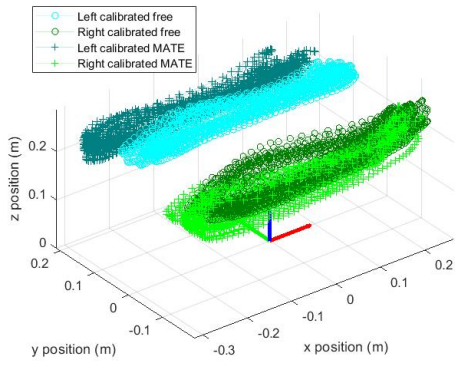


Fig. 13. Motion capture data from the left and right leg attachment points, both with and without the MATE, transformed

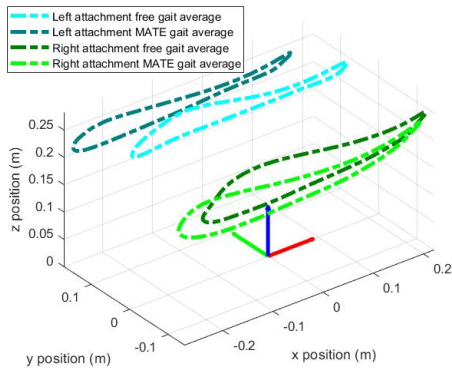


Fig. 14. Average gait cycles of the motion capture data of the left and right leg attachment points, with and without the MATE

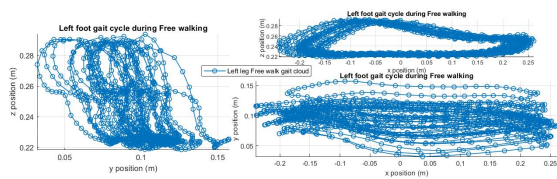


Fig. 15. Motion capture data from the left leg attachment point, without the MATE, transformed

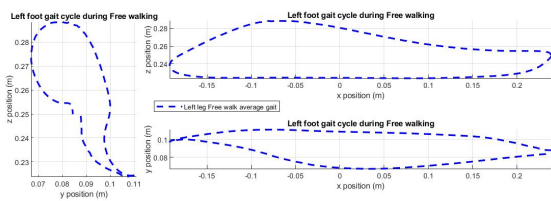


Fig. 16. Average gait cycle of the motion capture data of the left leg attachment point, without the MATE

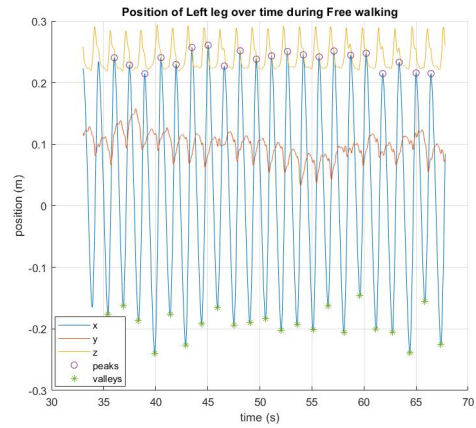


Fig. 17. Cartesian positions of the left leg motion tracker during the duration of free walking

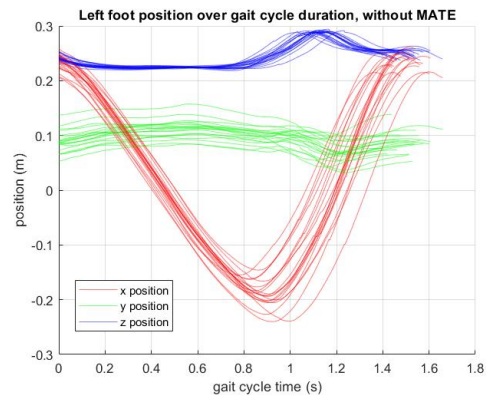


Fig. 18. Cartesian positions of the left leg motion tracker separated into different steps

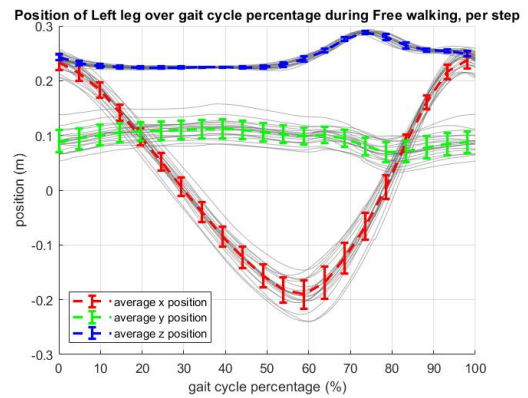


Fig. 19. Cartesian positions of the left leg motion tracker averaged over gait cycle percentage

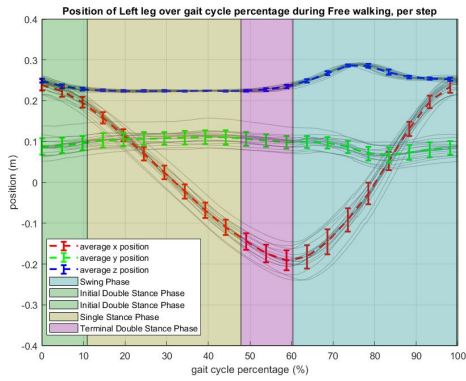


Fig. 20. Cartesian positions of the left leg motion tracker averaged over gait cycle percentage with gait phase

In addition to the spatio-temporal correspondence, forces were evaluated over the gait cycle. The full force sensor output can be seen in [Figure 22](#), the walking period is extracted and seen in [Figure 23](#). A single step is seen in [Figure 24](#) and all steps are averaged to [Figure 25](#). The gait phases are shown in addition to these forces in [Figure 26](#). The average force is divided by the weight of the participant and decomposed into Cartesian directions, see [Figure 27](#). These are compared to the threshold in [Figure 28](#). Larger versions of most of these figures can be found in [section F](#)

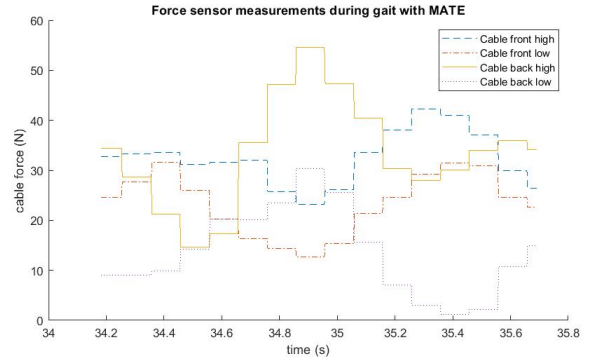


Fig. 24. Force sensor output over a single step

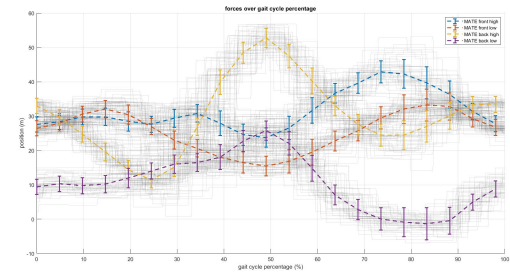


Fig. 25. Force sensor output averaged over gait cycle

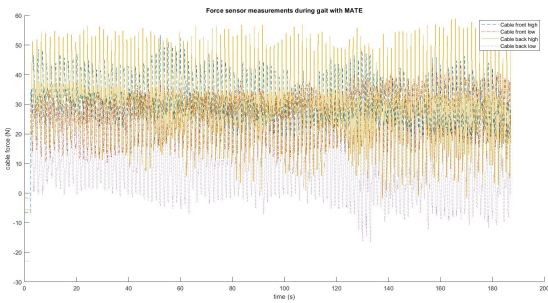


Fig. 22. Force sensor output over the entire human experiment

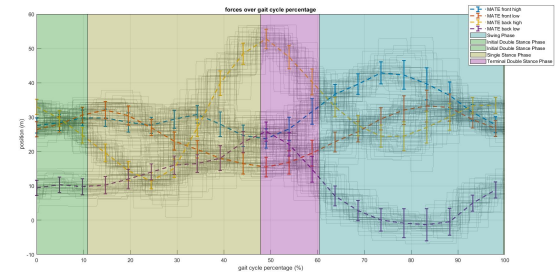


Fig. 26. Force sensor output averaged over gait cycle with gait phases

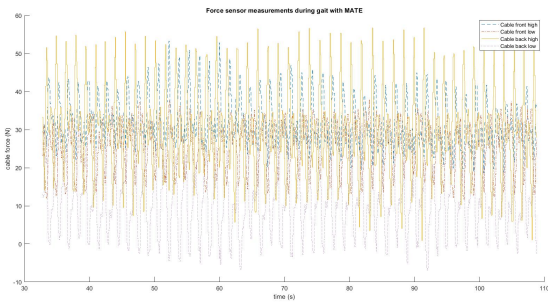


Fig. 23. Force sensor output while the participant is walking on a constant treadmill velocity

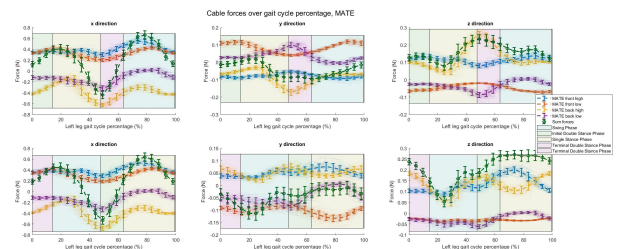


Fig. 27. Forces acting on the legs in the x and z direction, from the individual cables and their sum

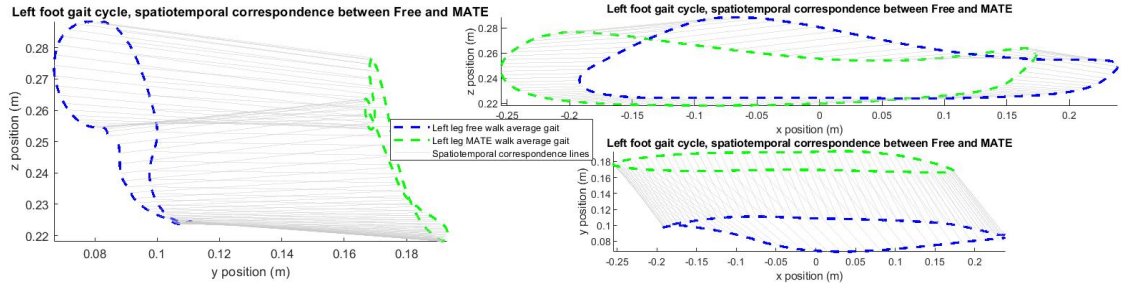


Fig. 21. Spatio-temporal correspondence between walking free and with MATE for left leg tracker, averaged gait cycle

*[t]

TABLE V
SPATIO TEMPORAL METRICS WITH STANDARD DEVIATIONS OF THE DIFFERENT GAIT CYCLES

Metric	Gait cycle			
	Left Free	Right Free	Left MATE	Right MATE
Step Length (m)	0.439 ± 0.028	0.460 ± 0.023	0.440 ± 0.036	0.501 ± 0.031
Stride Length (m)	0.899 ± 0.037	0.899 ± 0.037	0.940 ± 0.034	0.940 ± 0.034
Step Height (m)	0.048 ± 0.012	0.036 ± 0.010	0.040 ± 0.014	0.042 ± 0.013
Stride Width (m)	0.198 ± 0.011	0.198 ± 0.012	0.192 ± 0.011	0.292 ± 0.014
Step Duration (s)	0.733 ± 0.031	0.794 ± 0.032	0.751 ± 0.029	0.815 ± 0.033
Stride duration (s)	1.53 ± 0.047	1.53 ± 0.047	1.57 ± 0.048	1.57 ± 0.048
Stance Percentage (%)	60.6 ± 1.3	63.3 ± 1.6	64.0 ± 2.8	66.8 ± 1.9
Swing Percentage (%)	39.1 ± 1.3	36.7 ± 1.6	36.0 ± 2.8	33.2 ± 1.9
Double Limb Support Percentage Initial Stance (%)	11.3 ± 1.6	12.7 ± 1.4	14.7 ± 2.2	16.0 ± 3.0
Double Limb Support Percentage Terminal Stance (%)	12.5 ± 1.4	11.2 ± 1.5	16.0 ± 2.9	14.7 ± 2.1
Single Limb Support Percentage (%)	36.8 ± 1.1	39.5 ± 1.1	33.3 ± 1.9	36.1 ± 2.9

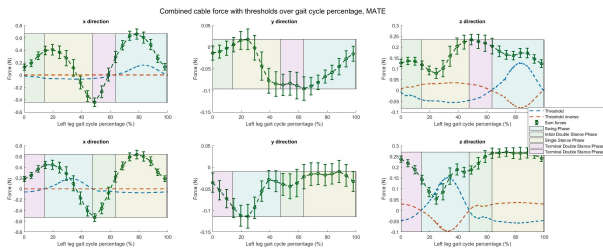


Fig. 28. Sum of cable forces compared to threshold forces as determined by [21]

The participant made the following comments after finishing the experiment:

- Left front lower pulley (f_{l1}) seemed to pull harder
- MATE felt comfortable to wear during the experiment
- MATE was not easy to attach
- Forces seemed to act in the right direction, assistive

V. DISCUSSION

A. MATE Design Properties

With the design of the MATE as is, there are several properties that can be advantages and disadvantages based on the application.

Advantages include that the length of the cables can be customized due to the method of attachment. On one side of the leg, opposing the side that connects to force sensors, the cable forms a loop. The cable is then clamped to itself and cannot shift. Loosening this clamp allows the loop to shrink

or grow, increasing and decreasing the effective length of the cable respectively. This can also be used to set the pretension in each cable.

Because the patient is only connected to the MATE with the cuff and cables, there are no rigid connections. The cables also add minimal weight to the body and have much less inertia as compared to robots that use orthoses [33], thus if the cables are slack there is minimal impedance to a patients natural gait.

The cost of the device is much less than alternatives. The design as is, not including the BWS and treadmill, can be produced for a few hundred euros material cost.

A disadvantage is that the pulley configuration is limited to the range of the frame. The frame has been designed so that the y-z axes of the frame can be fully utilized for placing the pulleys, but the x position of the pulleys is set, see Figure 2. This is in part due to the connection with the Lokomat and the Lokomat treadmill. Although a more complex frame design allows for movement of the x position of the pulleys, the effective gain in performance was expected to be low compared to the increased complexity of the frame. This was also done to reduce the amount of variables in the optimization problem in [20].

Because there are no actuators in the MATE, there is no predefined gait that the MATE aligns the patient with. The forces depend on the absolute positions of the legs, the pulleys and the stiffness of the cables. The configuration of the MATE cannot be altered while it is attached, so there is no real-time adjustment to the forces.

The cable stiffness was assumed constant at 300 N/m but turned out to more resemble 160 N/m. So the stiffness of the

cable as extracted from datasheets is not reliable and must be tested. Furthermore, the cable has non linearities that should not be neglected if the elongation difference is more than 10 %.

The friction in the pulleys was assumed negligible after literature research. The Coulomb friction was expected to be dominant but not too much. The Coulomb friction was not high, but there seemed to be large viscous friction that is not negligible.

B. Lokomat

The motion capture calibration seems to align the movement with the global coordinate system. The duration of the Lokomat experiment is much shorter, which would reduce the possibility of large drift.

The variance of the position of the end effectors is very consistent between gait cycles. Looking at [Figure 4](#) and [Figure 6](#), it can be seen that the Lokomat provides a stable gait as expected. There is a large but consistent difference between the forward kinematic estimate and the motion capture data. Part of the difference in the x-axis is explained because the tracker is placed slightly in front of the shin. This is about a 5 cm difference at most looking at the thickness of the tracker and Lokomat. The measured difference of 15 cm must also have another source. The forward kinematics might not be properly configured. The difference in the y-axis seems to be very consistent over time which could indicate a difference in the y-axis definition. This could be an error in the calibration or in the forward kinematics setup.

The data of the motion capture had similar variance to the data from the forward kinematics. It was discovered that the knees of the Lokomat were not properly tightened and allow for a rotation around its axis. As the tracker was placed around this axis, this free rotation could cause variance, but as the tracker was placed close to this rotation axis the variance would be small.

The forward kinematics work well in the range of values encountered during the predetermined gait. However, deviating from this gait too far back, or having a too large rotation in the knee, stops the code. This is because one of the needed intersections becomes mathematically impossible, further indicating an error in the forward kinematics. The forward kinematics is based on intersections of circles. Reforming this using existing packages or with other formulas could solve this issue.

The forces were also very consistent between gait cycles. The forces of cables 3 and 4 were much larger than the forces of cables 1 and 2. The expected elongation during the gait cycle was below 10%, which would correspond to a force of at most 30 N. Cables 3 and 4 surpass this value. This is likely from pretension in those cables or that the gait was further to the front than expected.

As the Lokomat has a high stiffness, the gait should not be altered with the addition of the MATE. Thus, this force decomposition is for a consistent gait, where that of the human experiment might be changed depending on the effect of the MATE. This seems to be confirmed by the similarity in the gait with and without the MATE, see [Figure 4](#). However, the knee

stiffness is not optimally tuned and can introduce an error of the same order as the error due to the motion capture system.

The forces surpass the threshold almost exclusively. This would indicate that the forces applied by the MATE would alter a healthy gait. However, there are questions about the validity of these thresholds. In their original use case, these thresholds were used to induce altered gaits by applying these forces at different points during the gait cycle, which is different from the constantly present applied force of the MATE. The thresholds might still serve as an indication whether the size of the forces is in the right order of magnitude.

The force combination averaged seems to indicate similar forces, but the actual forces would be different. The standard deviation seems smaller than expected, it seems there is an error in the code. The average still helps with estimating the force, especially with how much it exceeds the threshold.

C. Human

When looking at the data for the motion capture with the human experiments, no results can directly be made from the spatio-temporal correspondence. Before that, the process of gathering data and the preliminary results seem to be working well.

The difference between the two transformation matrices, both pre and post experiment, are small so little drift has taken place and tracker information is an unlikely cause for the differences seen. The only exception is the z value, which has shifted downwards from 18 cm cm too high to 11 cm cm too high. This was only 2 cm in the x direction and 3 cm in the y direction. These changes could either be a result of drift in the tracker or the tracker shifted on the body. Physical inspection of the tracker placement during the experiment did not notice change in placement, but the participant noted it felt like the tracker shifted. The newly designed cable attachment was not implemented and cannot be confirmed to remedy these issues.

The amount of data collected by walking forty (40) seconds instead of two (2) minutes was enough to perform all the calculations with. The walking time was reduced during the experiment.

The peak analysis and averaging code resulted in seemingly accurate gait cycle averages. Looking at the spatio-temporal correspondence between the free walking and walking with the MATE leads to some estimates, even though no method to compare them mathematically has been used. The average gait duration with and without the MATE is very similar. The 2.9% increase in duration will not be further taken into account.

Looking at the xy plane for both legs, the stride or step length seems to be the same. [Figure IV-B](#) gives values for the difference in maximum stride length of 2 cm for the left leg and 4 cm for the right leg. The height of the step changed in the right leg, 4 mm, but more than twice as much in the left leg, 9 mm.

Walking with the MATE tends to be more backwards than walking free. For the left leg walking with the MATE was 6 cm further back, and with the right leg it was 4 cm. The height of the step is lower with the MATE, leading to a more compressed gait, which could cause dragging on the treadmill.

The largest deviation is between the y position of the left leg. There is almost a 10 cm difference between the average y position when walking with and without the MATE. This can in part be explained by a defect in the device. The pulley on the front left bottom seemed to be dragging according to the feeling of the participant. When investigating this pulley it did seem to have a higher amount of friction than the other pulleys and it would not rotate. The flat undersides of the gaits should be at the same height, as those are made when the foot is flat on the treadmill. The deviation seen in the calibration is also seen here, such that the gait with the MATE is lower than the gait walking freely. This could be the drift in the sensor or the tracker itself could have moved, as it should be at the same height in both scenarios.

The sum of the forces almost exclusively exceeds the determined threshold values. This should indicate a large deviation in the stride length, but none was detected. This indicates that the method these thresholds are determined with are not valid in this scenario. The individual cable forces never cross 0, which indicates that no cable went slack during the walk and that the pretension was sufficient. Lower pretension would apply lower forces during the walk, but that counts for both parasitic and assistive forces. While the individual forces do not cross 0, the sum of the forces can be both positive and negative and changes over the gait cycle.

These forces were applied at the same points on both legs. The high cables were attached to the inside and the low cables attached to the outside. Different placements of these attachments might lead to a different level of control over the movement of the legs, comparing the used placement to [14] where the forces are applied near the ankle and the knee.

The 0 force readings from the pre and post experiment calibration indicated little effect from sensor bias and drift. The drift is assumed linear over the amount of time the force sensors have non-zero load applied to them.

The participant noticed that walking more forwards on the treadmill increased the difficulty and walking more towards the back introduced imbalance. The second scenario should be avoided by reducing the possibility of walking too far back. For this an assistive back pillow could be used, as it prevents walking back but not to the front. This pillow should be mounted on a spring system or with another non-rigid connection to reduce the impact force as the person moves backwards on the treadmill. The observation that walking forwards is more difficult could be used as a method of training and might be worth looking further into.

After the MATE was removed, the participant mentioned feeling some after effects. This indicates that the participant was adjusting to the MATE, which could be detrimental to its use in rehabilitation if the adjustment is to a non physiological gait pattern.

D. Limitations

Some assumptions were made during the design of the MATE. These can introduce errors into the system. One of these is the simplified effect of the cable elasticity. It is assumed linear, but validation shows that there are non-

linearities in the cable elasticity [B]. Furthermore, the assumed stiffness is higher than the actual stiffness measured.

Also, the calculations do not account for friction. Preliminary literature investigations led to the estimated effect being low. The performed validation showed that this friction is non-negligible [A]. One of the pulleys was found to be faulty and non-rotating, causing high friction that should not have been neglected. This pulley has since been replaced.

There was only one (1) participant with the human experiment and only the Lokomat for reference. The experiences of this participant are unlikely to be universal, and thus a larger sample size is needed.

The attachment of the cables is not ergonomic. They have been designed to be functional for the purpose of experiments but not for the long-term comfort of its wearers. A new cable attachment has been designed and built, see [B]. Due to a broken sensor, this attachment has not been included in new experiments and has not been investigated to solve these issues.

The cable placement has not been researched. A point on the shin halfway the knee and ankle was chosen as the position. No other placements have been investigated. Putting all the cables on the same point, such as the ankle, or placing the cables on different points, such as the ankle and the knee, might lead to different levels of control.

The threshold values do not make sense for this application.

The optimal amount of pretension is as yet undetermined. The configuration of the cables resembles a closed circuit cable/pulley drive, of which the recommended pretension is half of the estimated maximum tension [34]. Depending on the variance between people or how much the path can deviate from the test gait, the pretension might need to be increased.

E. Recommendations

The forward kinematics have been implemented from a previous paper [31]. To the authors knowledge no validation of these kinematics have been performed. There are several differences between motion capture and forward kinematics and it is currently unknown which, if not both, of these methods introduces this difference.

See if different cable placements affect the efficacy of the MATE. Possibly attach one pair of cables (front and back) at the knee and the other at the ankles, similar to the placement in [14].

Investigate different placement of the pulley. The optimal parameters were different for each participant in [20]. Generalizing an optimum between participants leads to a constant design, but if a method were designed that could estimate the optimal placement of the pulleys based on the physical properties of the participant the MATE might improve.

Investigate the possibility to use linear elastic element with non-elastic cable. The effects of elastic cables in this system introduce unknown variables and their stiffness is not linear. It has been determined that during a healthy gait cycle the geometry could allow for this depending on the size of the elastic element. There are sections of rope that do not pass over the pulley. If there are errors in the gait cycle, this section

might be smaller or not exist, which would cause the elastic element to pass over the pulley. Placing the frame further away from the centre of the treadmill elongates the cables and increases the range where a series elastic element would fit. Use the cables for further preliminary studies and investigate the series elastic element for a more finalised design.

For these experiments, different computers were needed to collect the data and run the treadmill. For ease of use and to allow real-time interaction between the software, run everything on a single computer. Furthermore, the frequency at which the force sensor data is stored should be increased to be at least faster than the Unity frequency so no data gets lost. This can be done in the LabView code. It has been tested up to 200 Hz without errors in [subsection A](#).

The force sensors are more fragile than anticipated. One broke during testing and had to be replaced. They have been secured more now, but extra care should be taken in any future testing.

The pulleys were modified by hand to increase the diameter of cables that would fit. This led to the faulty pulley. Investigate whether other pulleys suffer from this issue. If possible, purchase single joint revolute pulleys suitable for thicker cables.

The method used to set the pretension is unreliable and needs to be modified. If the required force for pretension can be determined, possibly using [\[34\]](#), use the force sensor data to set the cables to this pretension.

VI. CONCLUSION

This research consisted of a preliminary investigation into the forces and effects of the MATE. It achieved this by implementing motion capture with force sensor data to investigate the attachment coordinates and the forces in Cartesian directions.

Using motion capture works well. Implementing pre and post experiment calibrations allows for accurate transformations over the entire gait.

The forces present during a healthy gait exceed the predetermined thresholds and affect the gait. A visual spatiotemporal analysis shows deviation from the healthy gait cycle when using the MATE. These deviations can be explained by several faults in the design, the largest deviation being due to a faulty pulley. Redesigning the MATE with this in mind will lead to a higher performance. According to the participant, the MATE felt assistive when faking a pathological gait and was comfortable to use.

The placements of the cables and pulleys are most likely sub-optimal and affect the performance of the MATE.

The MATE in its current form does not function to the required level. Taking redesign and faults during the experiments into account, future iterations of the MATE can likely achieve this quality.

ACKNOWLEDGMENTS

The author would like to thank their supervisors from the TU Delft for their advice during the weekly meetings. Thank you Laura Marchal Crespo and Heike Vallery. Further the

PHD'ers who assisted with the thesis, mostly with getting the Lokomat working. Thank you Alex van der Berg, Alex Raschat and Stefano Dalla Gasperina. Thank you Maurits Pfaff for all the work on the electronics of the Lokomat and Jos van Driel for the force sensors that so much of these experiments rely on. Thank you Jason Moore for lending the frame components that make up the MATE. Lastly, thank you Tessa Huizing, my lovely girlfriend who, even though she knows nothing of this report, was a great source of support.

REFERENCES

- [1] V. L. Feigin, M. Brainin, B. Norrving, S. Martins, R. L. Sacco, W. Hacke, M. Fisher, J. Pandian, and P. Lindsay, "World stroke organization (wso): Global stroke fact sheet 2022," *International Journal of Stroke*, vol. 17, pp. 18–29, 1 2022.
- [2] V. L. Feigin, B. A. Stark, C. O. Johnson, G. A. Roth, and C. Bisignano, "Global, regional, and national burden of stroke and its risk factors, 1990–2019: a systematic analysis for the global burden of disease study 2019," *The Lancet Neurology*, vol. 20, pp. 795–820, 10 2021.
- [3] B. Hobbs and P. Artemiadis, "A review of robot-assisted lower-limb stroke therapy: Unexplored paths and future directions in gait rehabilitation," *Frontiers in Neurobotics*, vol. 14, 4 2020.
- [4] P. Langhorne, F. Coupar, and A. Pollock, "Motor recovery after stroke: a systematic review," *The Lancet Neurology*, vol. 8, pp. 741–754, 8 2009.
- [5] G. E. Gresham, T. E. Fitzpatrick, P. A. Wolf, P. M. McNamara, W. B. Kannel, and T. R. Dawber, "Residual disability in survivors of stroke - the framingham study," *New England Journal of Medicine*, vol. 293, pp. 954–956, 11 1975.
- [6] M. F. Bruni, C. Melegari, M. C. D. Cola, A. Bramanti, P. Bramanti, and R. S. Calabro, "What does best evidence tell us about robotic gait rehabilitation in stroke patients: A systematic review and meta-analysis," *Journal of Clinical Neuroscience*, vol. 48, pp. 11–17, 2 2018.
- [7] J. J. Eng and P.-F. Tang, "Gait training strategies to optimize walking ability in people with stroke: a synthesis of the evidence," *Expert Review of Neurotherapeutics*, vol. 7, pp. 1417–1436, 10 2007.
- [8] S. Peurala, O. Airaksinen, P. Huuskonen, P. Jakala, M. Juhakoski, K. Sandell, I. Tarkka, and J. Sivenius, "Effects of intensive therapy using gait trainer or floor walking exercises early after stroke," *Journal of Rehabilitation Medicine*, vol. 41, pp. 166–173, 2009.
- [9] R. S. Calabro, A. Cacciola, F. BertÄs, A. Manuli, A. Leo, A. Bramanti, A. Naro, D. Milardi, and P. Bramanti, "Robotic gait rehabilitation and substitution devices in neurological disorders: where are we now?" *Neurological Sciences*, vol. 37, pp. 503–514, 4 2016.
- [10] C. Werner, S. von Frankenberg, T. Treig, M. Konrad, and S. Hesse, "Treadmill training with partial body weight support and an electromechanical gait trainer for restoration of gait in subacute stroke patients," *Stroke*, vol. 33, pp. 2895–2901, 12 2002.
- [11] J. Mehrholz, S. Thomas, J. Kugler, M. Pohl, and B. Elsner, "Electromechanical-assisted training for walking after stroke," *Cochrane Database of Systematic Reviews*, vol. 2020, 10 2020.
- [12] X. Zhang, Z. Yue, and J. Wang, "Robotics in lower-limb rehabilitation after stroke," *Behavioural Neurology*, vol. 2017, pp. 1–13, 2017.
- [13] X. Jin, A. Prado, and S. K. Agrawal, "Retraining of human gait - are lightweight cable-driven leg exoskeleton designs effective?" *IEEE Transactions on Neural Systems and Rehabilitation Engineering*, vol. 26, pp. 847–855, 4 2018.
- [14] Y. Zou, N. Wang, X. Wang, H. Ma, and K. Liu, "Design and experimental research of movable cable-driven lower limb rehabilitation robot," *IEEE Access*, vol. 7, pp. 2315–2326, 2019.
- [15] R. Hidayah, L. Bishop, X. Jin, S. Chamarthy, J. Stein, and S. K. Agrawal, "Gait adaptation using a cable-driven active leg exoskeleton (c-alex) with post-stroke participants," *IEEE Transactions on Neural Systems and Rehabilitation Engineering*, vol. 28, pp. 1984–1993, 9 2020.
- [16] R. Hidayah, S. Chamarthy, A. Shah, M. Fitzgerald-Maguire, and S. K. Agrawal, "Walking with augmented reality: A preliminary assessment of visual feedback with a cable-driven active leg exoskeleton (c-alex)," *IEEE Robotics and Automation Letters*, vol. 4, pp. 3948–3954, 10 2019.
- [17] R. Hidayah, X. Jin, S. Chamarthy, M. M. Fitzgerald, and S. K. Agrawal, "Comparing the performance of a cable-driven active leg exoskeleton (c-alex) over-ground and on a treadmill." *IEEE*, 8 2018, pp. 299–304.
- [18] Z. Qian and Z. Bi, "Recent development of rehabilitation robots," *Advances in Mechanical Engineering*, vol. 7, p. 563062, 1 2015.

- [19] M. Elarbi-Boudihir, "Rehabilitation robotics: a survey of issues and perspectives in the kingdom of saudi arabia," 2009.
- [20] B. Haanen, "A mate for post-stroke gait rehabilitation; design optimization of a minimally actuated tendon-based gait rehabilitation device," Master's thesis, 2022.
- [21] G. Severini, A. Koenig, C. Adans-Dester, I. Cajigas, V. C. Cheung, and P. Bonato, "Robot-driven locomotor perturbations reveal synergy-mediated, context-dependent feedforward and feedback mechanisms of adaptation," *Scientific Reports*, vol. 10, 12 2020.
- [22] D. P. Wyss, "Enabling balance training in robot-assisted gait rehabilitation," Ph.D. dissertation, 2019.
- [23] S. Fang, D. Franitza, M. Torlo, F. Bekes, and M. Hiller, "Motion control of a tendon-based parallel manipulator using optimal tension distribution," *IEEE/ASME Transactions on Mechatronics*, vol. 9, no. 3, pp. 561–568, 2004.
- [24] J. L. Emken, S. J. Harkema, J. A. Beres-Jones, C. K. Ferreira, and D. J. Reinkensmeyer, "Feasibility of manual teach-and-replay and continuous impedance shaping for robotic locomotor training following spinal cord injury," *IEEE Transactions on Biomedical Engineering*, vol. 55, pp. 322–334, 1 2008.
- [25] S. Maggioni, N. Reinert, L. L enenburger, and A. Melendez-Calderon, "An adaptive and hybrid end-point/joint impedance controller for lower limb exoskeletons," *Frontiers in Robotics and AI*, vol. 5, 10 2018.
- [26] J. S. Sulzer, M. A. Peshkin, and J. L. Patton, "Design of a mobile, inexpensive device for upper extremity rehabilitation at home."
- [27] B. Hu, F. Zhang, H. Lu, H. Zou, J. Yang, and H. Yu, "Design and assist-as-needed control of flexible elbow exoskeleton actuated by nonlinear series elastic cable driven mechanism," *Actuators*, vol. 10, 11 2021.
- [28] I. Marina. (2022) Heavy duty shock cord. [Online]. Available: <https://www.ibexmarina.com/portfolio-item/heavy-duty-shock-cord/>
- [29] D. C. Niehorster, L. Li, and M. Lappe, "The accuracy and precision of position and orientation tracking in the htc vive virtual reality system for scientific research," *i-Perception*, vol. 8, p. 204166951770820, 6 2017.
- [30] P. Bauer, W. Lienhart, and S. Jost, "Accuracy investigation of the pose determination of a vr system," *Sensors*, vol. 21, p. 1622, 2 2021.
- [31] D. Kluwen, "Kinematics analysis of an end-effector-based orthosis for the lower limb allowing for adduction and flexion," Master's thesis, 2022.
- [32] A. Kharb, V. Saini, Y. Jain, and S. Dhiman, "A review of gait cycle and its parameters," *IJCEM International Journal of Computational Engineering & Management*, vol. 13, pp. 78–83, 2011.
- [33] L. Marchal-Crespo and R. Riener, "Robot-assisted gait training," in *Rehabilitation robotics*. Elsevier, 2018, pp. 227–240.
- [34] E. R. Snow, "The load/deflection behavior of pretensioned cable/pulley transmission mechanisms onetlc4 it i k'9 l 3nd es," 1986, test note.

APPENDIX

APPENDIX A
FORCE SENSORS

Custom sensors were used to measure the tension in the cable. These were produced by the TU Delft measurement lab. The signals are transferred to Scaime-CPJ boxes which amplify and filter the signals. From those, a NiDAQ reads the amplified signals and can connect to the laptop. A Labview program processes the signals and saves them to an askii file, which can be converted to excel or matlab.

These sensors are made inhouse, no large scale validation is present. Thus, to use these a validation was performed. Weights were suspended from these sensors up to 30 kg in increments of 5 kg, resulting in [Figure 29](#). It can be seen that these curves are very linear. The linear fits have an R^2 value of 0.999 or above, so highly linear. The parameters of these linear estimations are used to convert measured voltage to force.

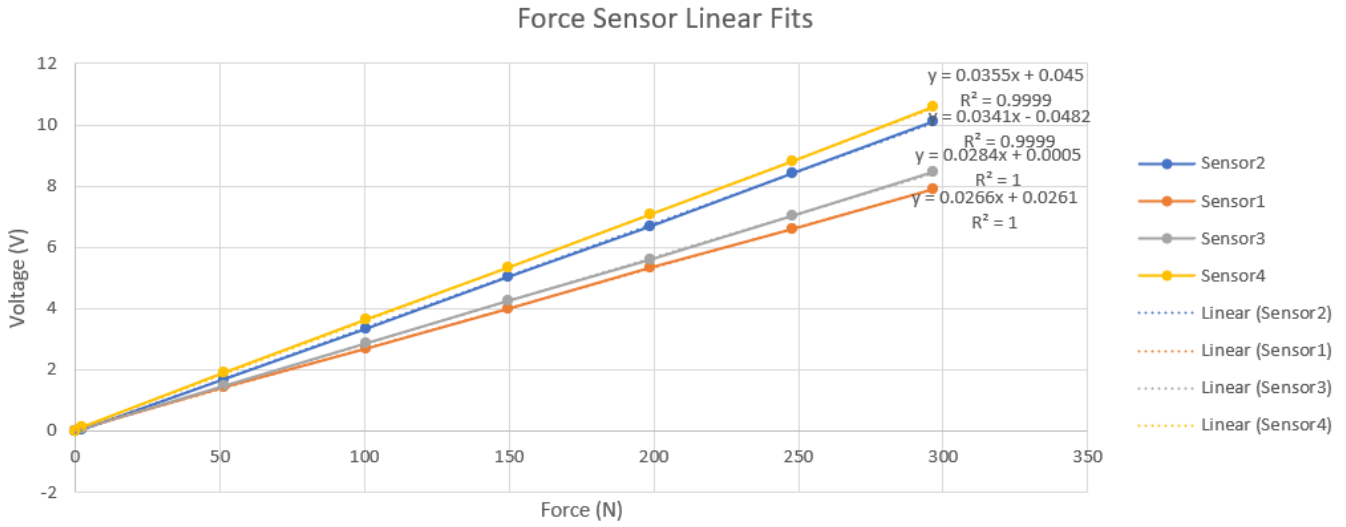


Fig. 29. Voltage over weight curves of the force sensors

A further investigation was performed to validate the bias of these sensors. To see whether the linear fit would fit well, again weights up to 30 kg in increments of 5 kg were suspended from a sensor. The constant forces, removing transitional periods, at each weight were averaged and compared between before and after suspending weights. This resulted in [Figure 30](#). A small bias was detected, so pre and post experiment calibrations will be performed to account for this bias.

Accounting for this bias happens after measurements have been taken. The change in bias is assumed to increase linearly over the time weight is put on the sensors. So when the cables are attached and recording starts, the bias is assumed to start shifting. Thus, over the duration of the measured walk, only a part of this bias is changed.

$$\Delta \text{bias} = \text{bias}_{\text{pre}} - \text{bias}_{\text{post}} \quad (4)$$

Where Δbias is the difference in the zero-weight measurements, $\text{bias}_{\text{post}}$ is the post-experiment zero-weight measurement and bias_{pre} is the pre-experiment zero-weight measurement. This bias is made to increase linearly over time with:

$$\text{slope}_{\vec{\text{bias}}} = \Delta \text{bias} / T_{\text{total}} * T_{\text{used}} \quad (5)$$

Where $\text{slope}_{\vec{\text{bias}}}$ is the linear slope of the bias as a vector of the entire used time, T_{total} is the total time non-zero forces were applied and T_{used} is a time vector of the walking period. The values of the force sensors have their pre-experiment bias removed and the linear slope added and are then converted to Newtons:

$$F_{\text{cable}} = (F_0 - \text{bias}_{\text{pre}} + \text{slope}_{\vec{\text{bias}}}) / a_{\text{con}} \quad (6)$$

Where F_{cable} is the cable force in Newtons, F_0 is the measured cable force in Volts and a_{con} is the conversion factor from Volts to Newton which is individual for each sensor. It is the multiplication factor of the slope in [Figure 29](#).

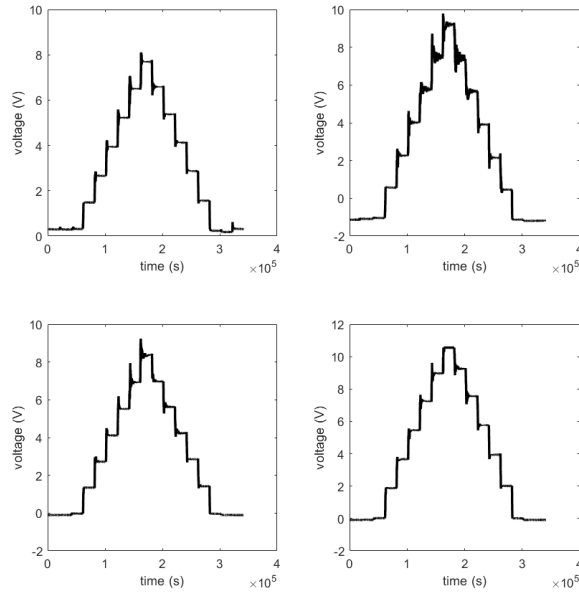


Fig. 30. Voltage over time curves of the force sensors to check for bias

APPENDIX B CABLE

A. Diameter Determination

From the dimensions as determined by Bram, the cables' length is approximately 2 m. The precise length varies per participant and setup, for each of the six (6) participants from the study of Bram Haanen the minimum and maximum length is denoted in [subsection II-C](#). For each cable the minimum length across all participants is taken as the unstretched length and the maximum length is used to determine the highest elongation. Datasheet of bungee cables for stiffness reference [subsection A](#).

TABLE VI

*: S8 ORIGINALLY, CORRECTED TO 58 **: VALUES SWITCHED TO CORRESPOND TO MIN AND MAX ***: 650 ORIGINALLY, CORRECTED TO 650

Diameter (mm)	10%	30%		75%		Total extension
	(Minimum)	Min	Max	Min	Max	
5	20N	29N	38N	50N	65N	105%
6.5	40N	[58]*N	76N	100N	130N	105%
8	60N	88N	116N	150N	196N	105%
9.5	80N	120N	170N	210N	280N	105%
12.5	150N	210N	280N	370N	480N	105%
16	240N	350N	460N	500N	600N **	105%
19	340N	500N	[650]**N	850N	1100N	105%
22	460N	660N	880N	1150N	1500N	105%

$$K = \frac{F}{\% * L} \quad (7)$$

where K is the stiffness, F is the force at given elongation from [subsection A](#), $\%$ is the elongation at which that force is measured and L is the length of the cable

From [Equation A](#) it is clear to see that the stiffness is not constant. Rather, it decreases with larger elongations. The needed stiffness is around 300 N/m for elongations of up to 10%. Including elongation from pre-tensioning the cables, the 8 mm diameter was deemed to be best fitting.

B. Stiffness

The 8 mm cable was purchased. To validate the stiffness, a set of weights were mounted to the cable and the stretch measured, see [Figure 31](#). This will be done for ten (10) cycles, increasing the weight from 0 to 3 kg and back to 0. This results in the curve [Figure 32](#) which is averaged to [Figure 33](#). The linear estimated stiffness of this final curve is approximately 160 N/m rather than the expected 300 N/m.

TABLE VII
DATASHEET OF BUNGEE CABLE STIFFNESS PER METER LENGTH OF CABLE

Diameter (mm)	10%	30%		75%		Total extension
	(Minimum)	Min	Max	Min	Max	
5	200N/m	97N/m	127N/m	67N/m	87N/m	105%
6.5	400N/m	193N/m	253N/m	133N/m	173N/m	105%
8	600N/m	293N/m	387N/m	200N/m	261N/m	105%
9.5	800N/m	400N/m	567N/m	280N/m	373N/m	105%
12.5	1500N/m	700N/m	933N/m	493N/m	640N/m	105%
16	2400N/m	1167N/m	1533N/m	667N/m	800N/m	105%
19	3400N/m	1667N/m	2167N/m	1133N/m	1467N/m	105%
22	4600N/m	2200N/m	2933N/m	1533N/m	2000N/m	105%

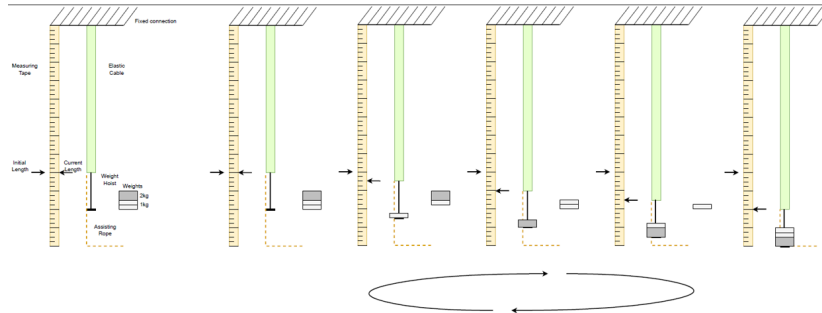


Fig. 31. Image of experiment setup of stiffness measure

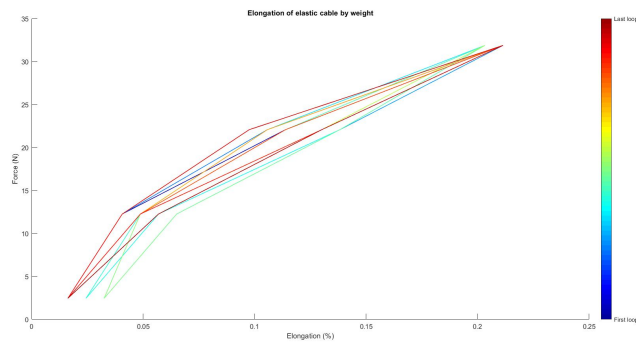


Fig. 32. Force over elongation curve, showing hysteresis

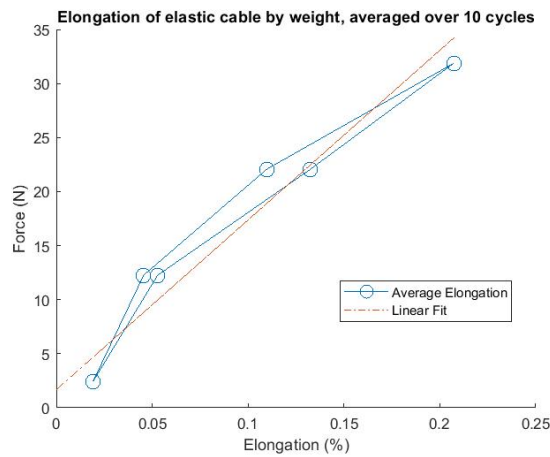


Fig. 33. Average force over elongation curve, showing hysteresis

APPENDIX C MATE

A. Pulley friction

In order to investigate the friction of the pulleys, a short validation was performed. One of the elastic cables is set to run over two pulleys and is attached to a force sensor with motion tracker on each end, see [Figure 34](#). Each end of the cable is moved, causing elongation of the cables and a resulting force. These are measured by the force sensors, see [Figure 35](#). The two sensors switch sides and again both ends of the cable are moved and pulled. The forces over time show that the forces are similar, but often one lags or overshoots the other. The forces are plotted against each other, see [Figure 36](#). Initially this showed a wide spread, but when colouring the data points according to the velocity of the cable a clear pattern emerges. The data points lie on two linear graphs, one for each direction of movement of the cable. As the friction opposes movement, these graphs seem to indicate viscous friction. Viscous friction was neglected in calculations but shows a clear effect. To make the lines more clear, the data was smoothened so that the variance of the tracker measurements is lessened. Future iterations of the MATE should improve on their pulley design or account for friction in their calculations.

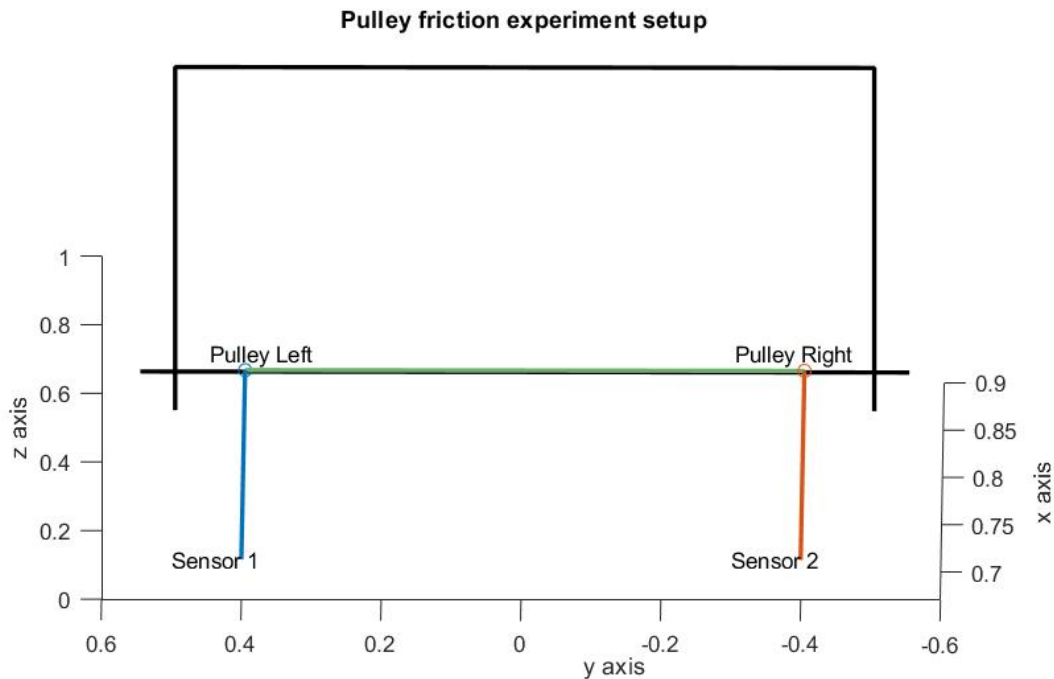


Fig. 34. Setup for the pulley friction experiment

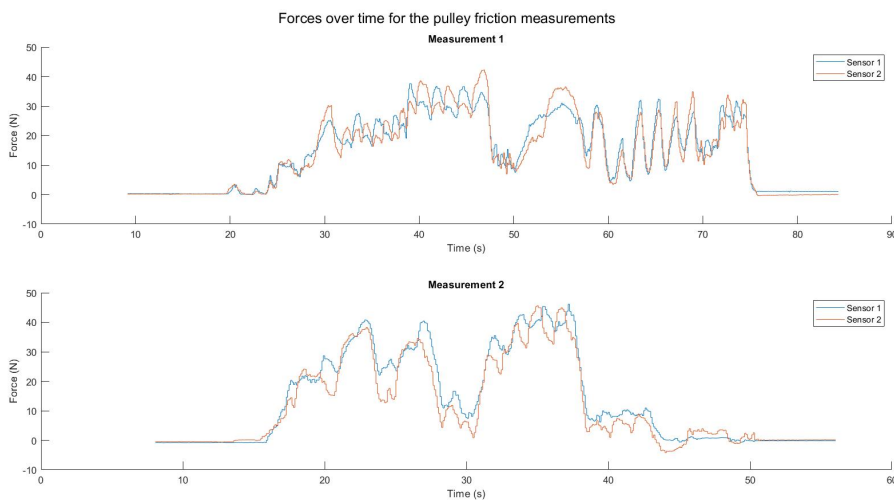


Fig. 35. Measured force sensor values over time

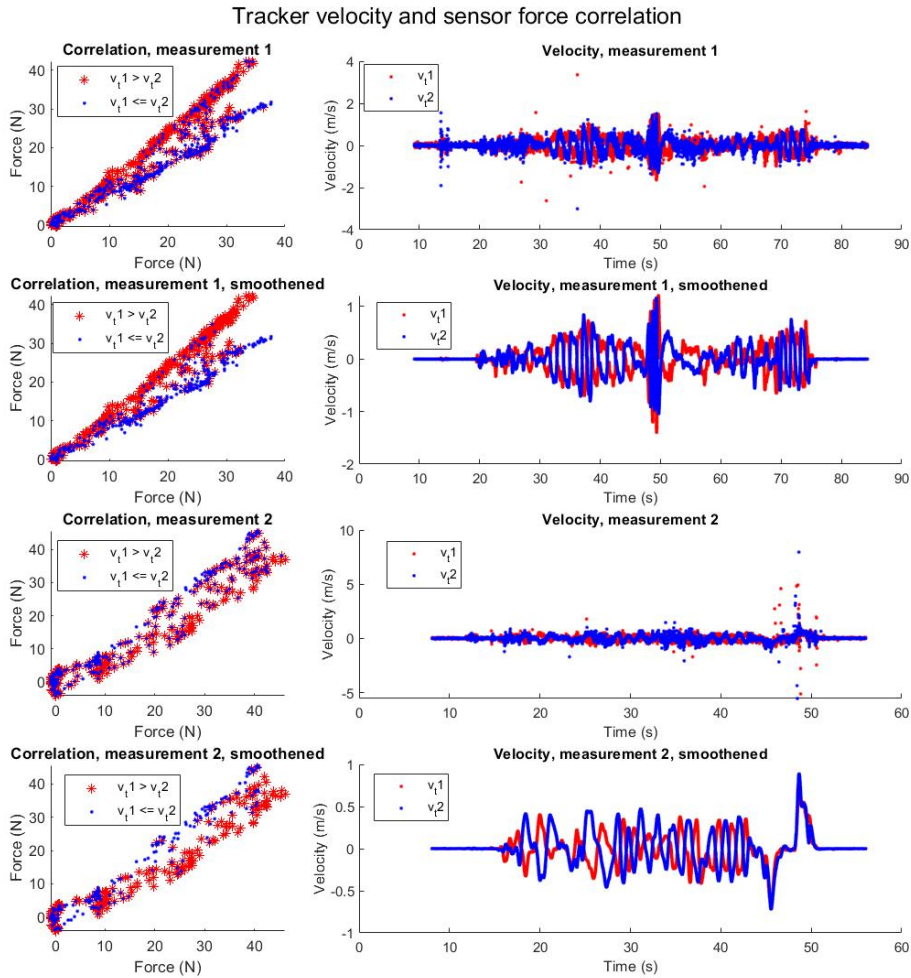


Fig. 36. Correlation force sensor measured forces and velocities over time

B. Attachment

The cable attachment has been redesigned. Instead of using the flexible cloth Velcro straps from the HTC VIVE, a metal attachment is used. This attachment has been built but not validated. It is made from 1 mm aluminium plate steel to check dimensions and keep it lightweight. The inside is lined with a foam to prevent damage to the legs. It is 6 cm high to account for the size of the tracker and 24 cm to account for attachment of the cable and the curve. First a plate must be made in the right dimensions. If a lasercutter is available, design a sketch similar to [Figure 37](#). If not, use a plate cutter and round the corners manually. The holes are all 5.0 mm. The outer two holes on each side are to connect bolts and nuts with. The inner two holes are to attach the cables to. The hole in the middle is 5.0 mm such that a M6 bolt without head can be tightened. If a plate with these holes is available, they must be curved. Using a plate roller these can be curved. Draw the right curve on a piece of paper and compare the made curve to this to ensure the right fit. Then bend the corners straight with a bending machine. Put the M6 inbus into the plate and glue the foam padding to the inside. During experimentation the 1 mm aluminium plate was able to bend too much, thicker plates or a redesign must be implemented to counter this.

APPENDIX D LOKOMAT JOINT SPACE DIFFERENCE

To determine the effect of the MATE on the Lokomat and check whether the Lokomat acts with a high stiffness, a joint space validation is performed. The ‘joints’ are all the values of the Lokomat output as explained in the Lokomat setup. Plotting these measurements for a single gait cycle results in [Figure 38](#). The difference between with and without the MATE can be seen in [Figure 39](#). For the pose of the pelvis no conclusions can be drawn as the recording failed. This could be because the light was obstructed or out of range. For the thigh actuators, the error is in the order of millimetres, less than the previously determined

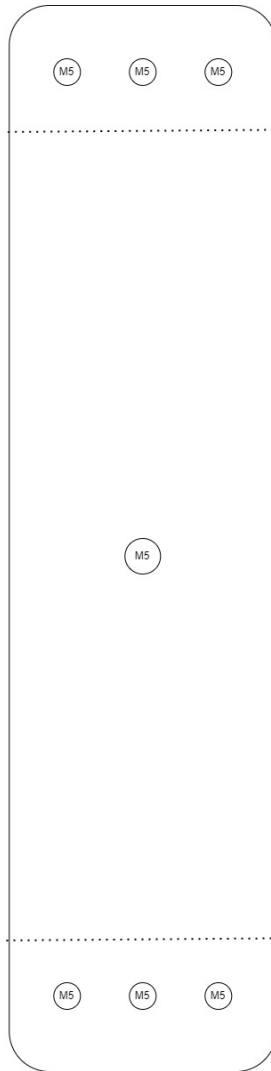


Fig. 37. 2d plate figure of the cable attachment design

accuracy of the trackers. The pelvis actuator also only has a difference of millimetres, but this is larger in comparison to its range of motion. The value indicates that the entire device was shifted slightly to the left. For the angles of the knees larger errors can be seen, especially when the knee goes to a small angle (extends). This happens when moving forward. Initially, the MATE seems to limit the angle, the graph flattens where Free still goes down. For the left leg the desired angle then matches the flattened and no large overshoot takes place. For the right leg, after first limiting the angle, there is an overshoot as the Lokomat tries to follow its path. From these results it seems that the Linear Actuator PD controller is tuned with a high stiffness but the gains of the knee controller are not properly tuned and is not stiff enough. Further tuning for the knee controller gains is recommended.

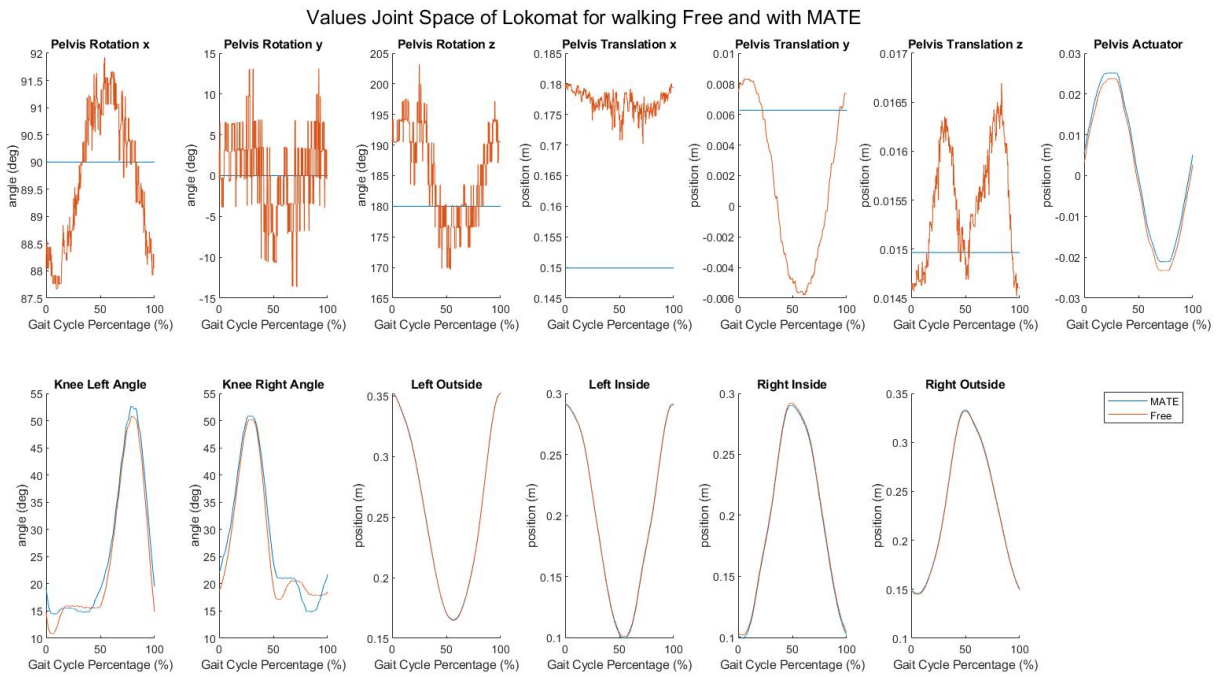


Fig. 38. Values Joint Space of Lokomat for walking Free and with MATE

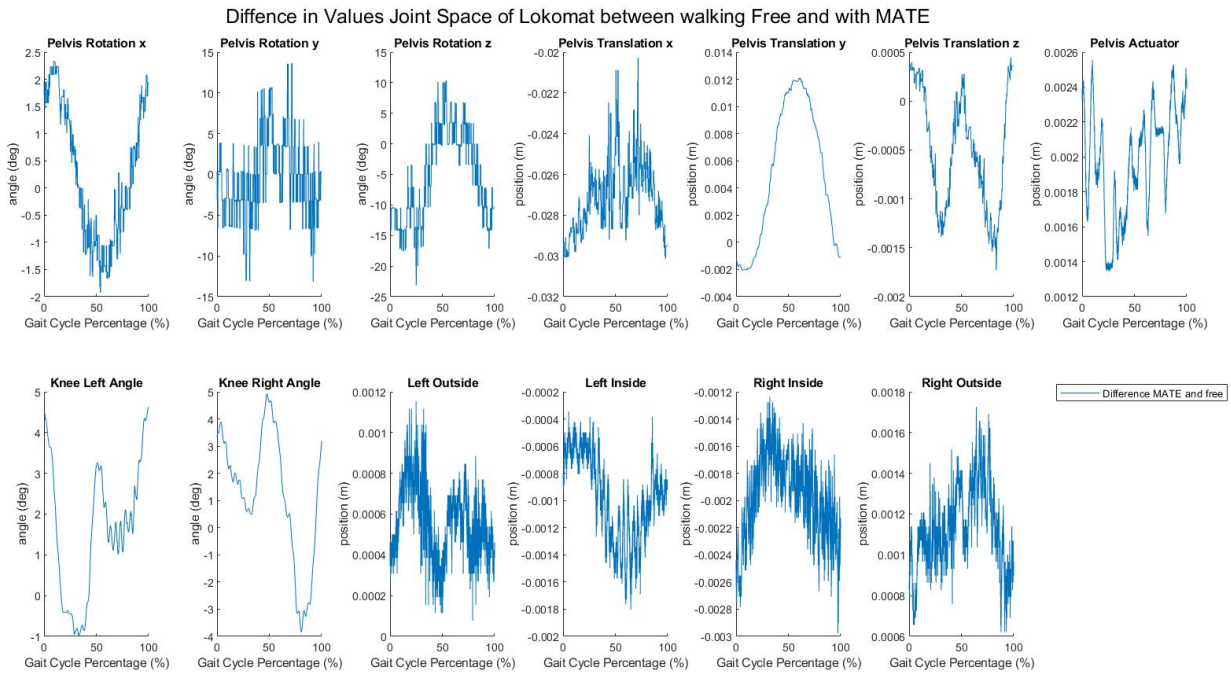


Fig. 39. Diffence in Values Joint Space of Lokomat between walking Free and with MATE

APPENDIX E LOKOMAT RESULTS EXPANDED

A. End Effector position

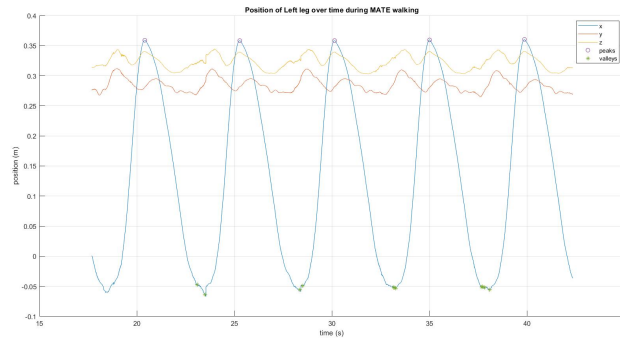


Fig. 40. Cartesian positions of the left leg motion tracker during the duration of walking with MATE

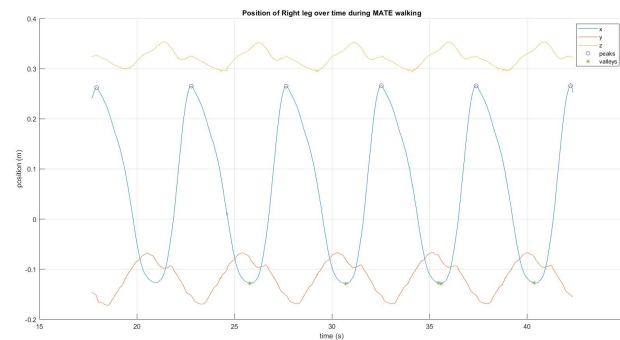


Fig. 41. Cartesian positions of the right leg motion tracker during the duration of walking with MATE

B. Split Gait

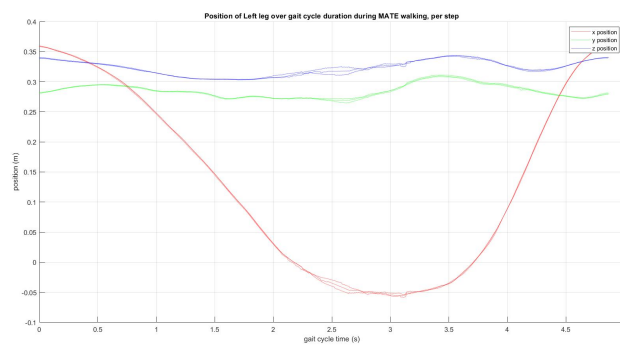


Fig. 42. Cartesian positions of the left leg motion tracker during walking with MATE separated into different steps

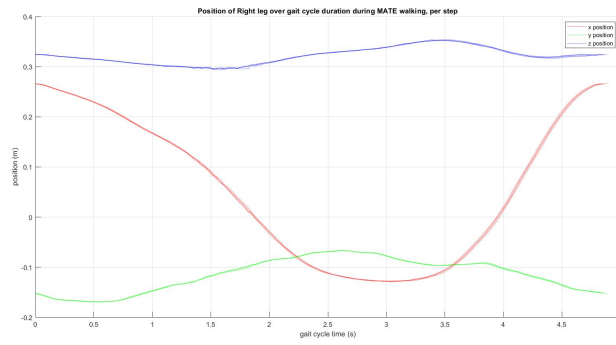


Fig. 43. Cartesian positions of the right leg motion tracker during walking with MATE separated into different steps

C. Averaged Gait

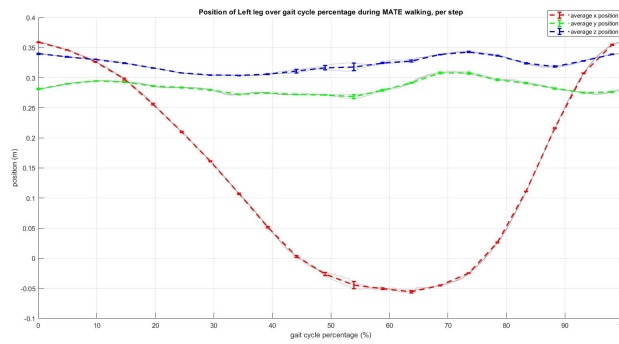


Fig. 44. Cartesian positions of the left leg motion tracker during MATE averaged over gait cycle percentage

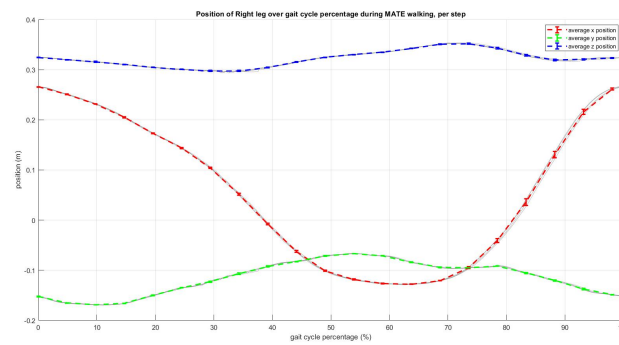


Fig. 45. Cartesian positions of the right leg motion tracker during MATE averaged over gait cycle percentage

D. Averaged Gait with Phases

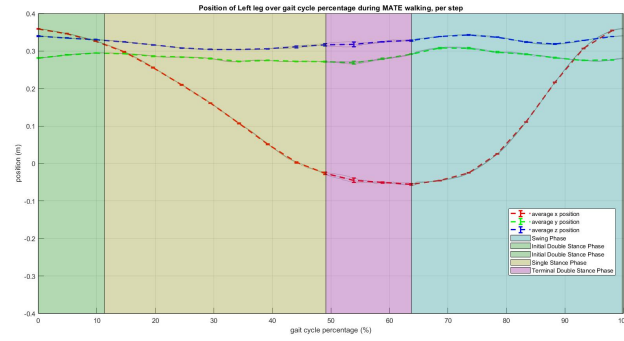


Fig. 46. Cartesian positions of the left leg motion tracker during MATE averaged over gait cycle percentage with gait phases

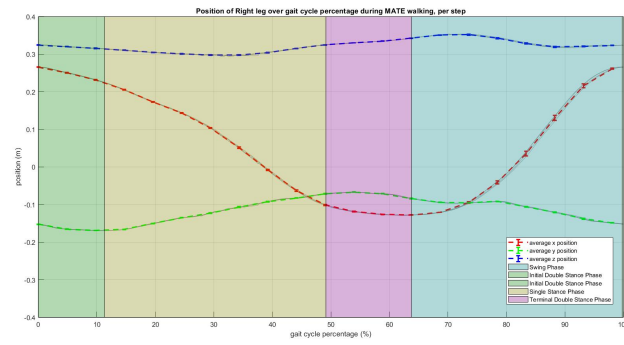


Fig. 47. Cartesian positions of the right leg motion tracker during MATE averaged over gait cycle percentage with gait phases

E. Forces

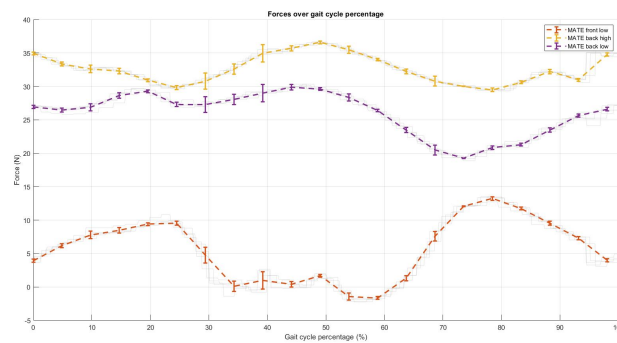


Fig. 48. Forces of the 3 working force sensors during MATE walking of the Lokomat

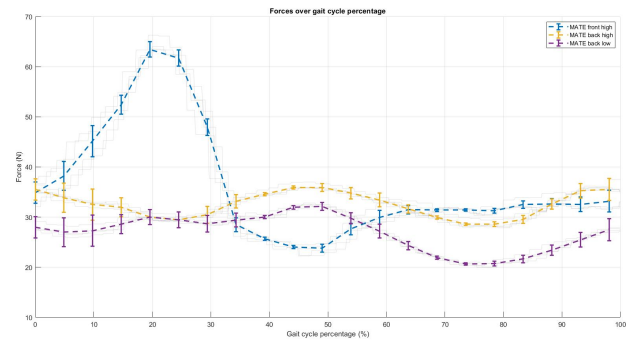


Fig. 49. Forces of the 3 working force sensors during MATE walking of the Lokomat

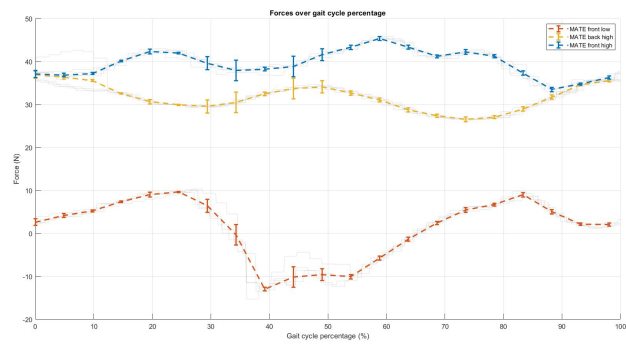


Fig. 50. Forces of the 3 working force sensors during MATE walking of the Lokomat

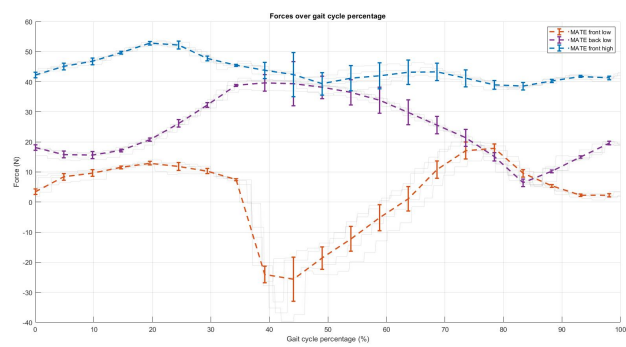


Fig. 51. Forces of the 3 working force sensors during MATE walking of the Lokomat

APPENDIX F
HUMAN RESULTS EXPANDED

A. Motion Capture Gait

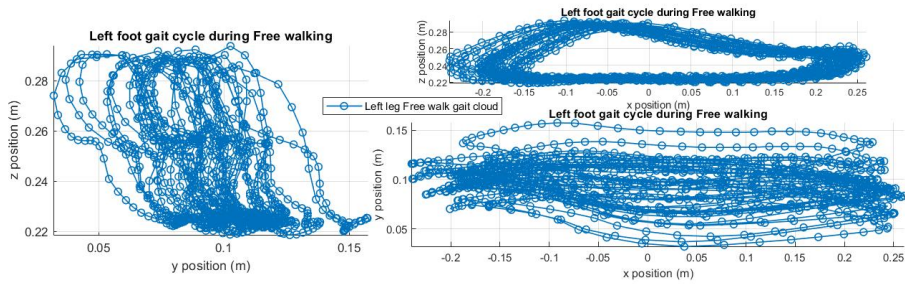


Fig. 52. Motion capture data from the left leg attachment point, without the MATE, transformed

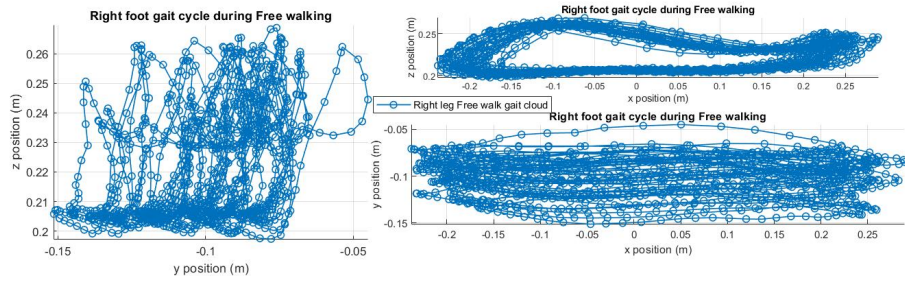


Fig. 53. Motion capture data from the right leg attachment point, without the MATE, transformed

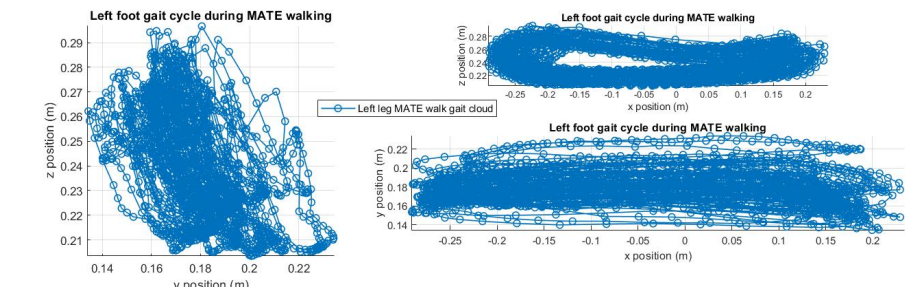


Fig. 54. Motion capture data from the left leg attachment point, with the MATE, transformed

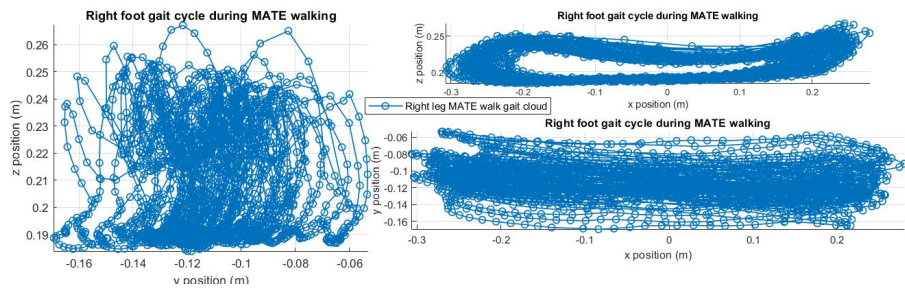


Fig. 55. Motion capture data from the right leg attachment point, with the MATE, transformed

B. Motion Capture Gait Average

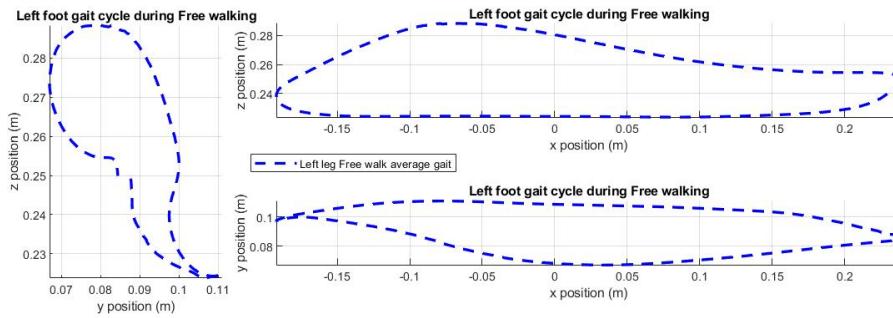


Fig. 56. Averaged motion capture data from the left leg attachment point, without the MATE, transformed

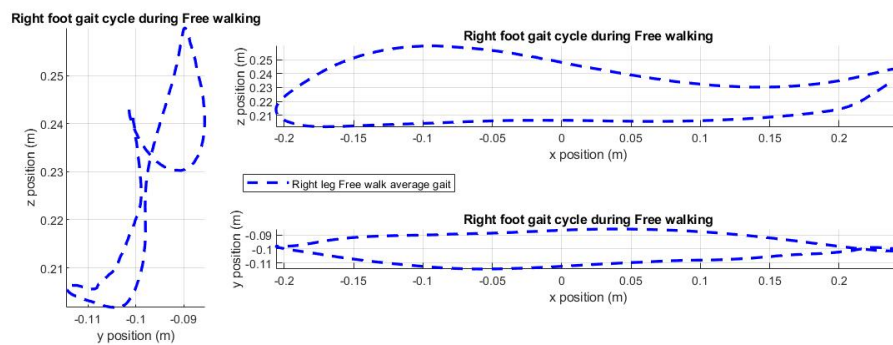


Fig. 57. Averaged motion capture data from the right leg attachment point, without the MATE, transformed

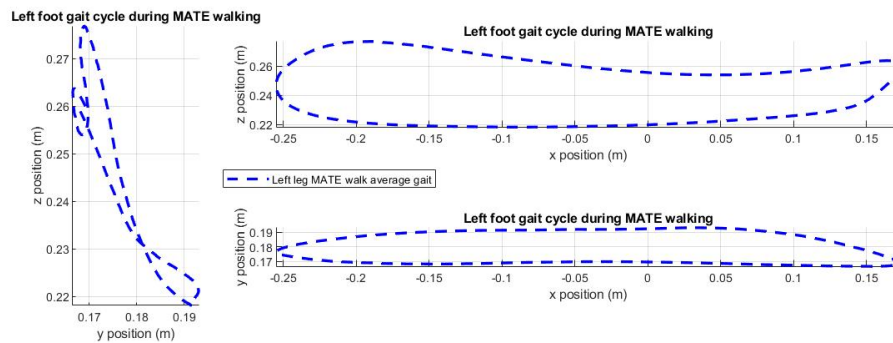


Fig. 58. Averaged motion capture data from the left leg attachment point, with the MATE, transformed

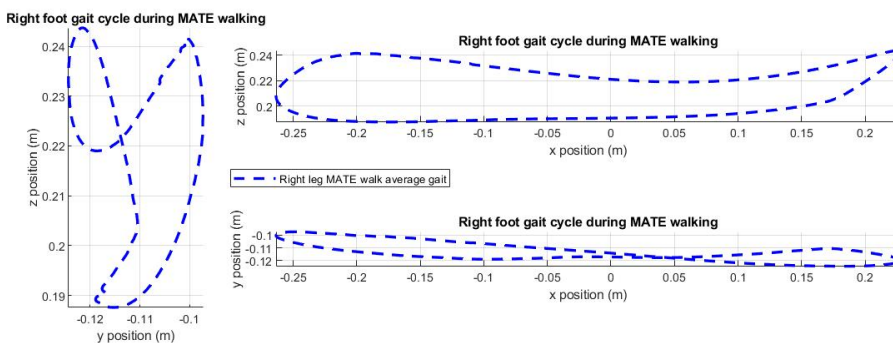


Fig. 59. Averaged motion capture data from the right leg attachment point, with the MATE, transformed

C. End Effector position

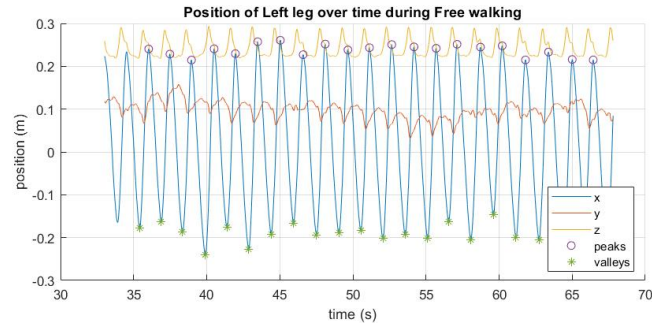


Fig. 60. Cartesian positions of the left leg motion tracker during the duration of free walking

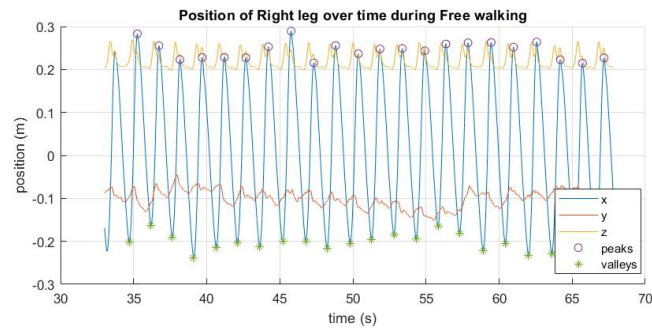


Fig. 61. Cartesian positions of the right leg motion tracker during the duration of free walking

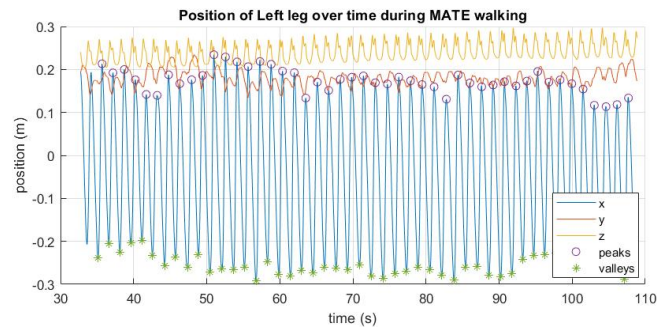


Fig. 62. Cartesian positions of the left leg motion tracker during the duration of MATE walking

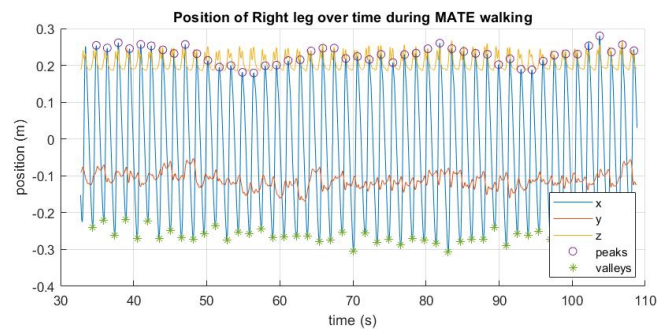


Fig. 63. Cartesian positions of the right leg motion tracker during the duration of MATE walking

D. Split Gait

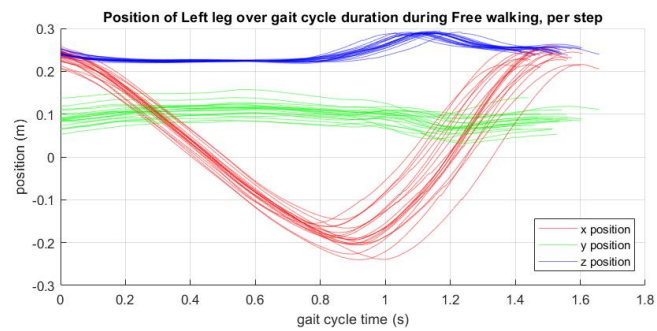


Fig. 64. Cartesian positions of the left leg motion tracker during free walking separated into different steps

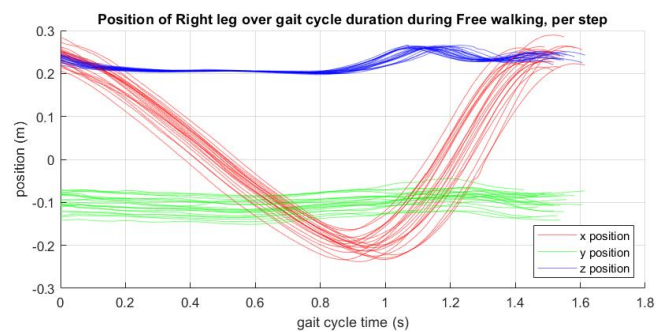


Fig. 65. Cartesian positions of the right leg motion tracker during free walking separated into different steps

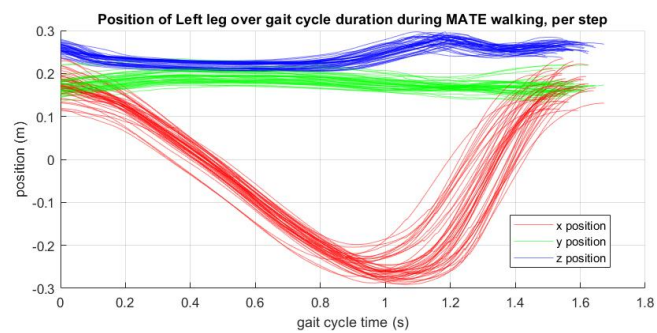


Fig. 66. Cartesian positions of the left leg motion tracker during MATE separated into different steps

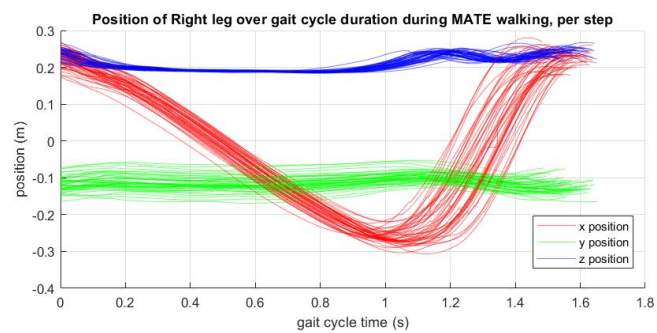


Fig. 67. Cartesian positions of the right leg motion tracker during MATE separated into different steps

E. Averaged Gait

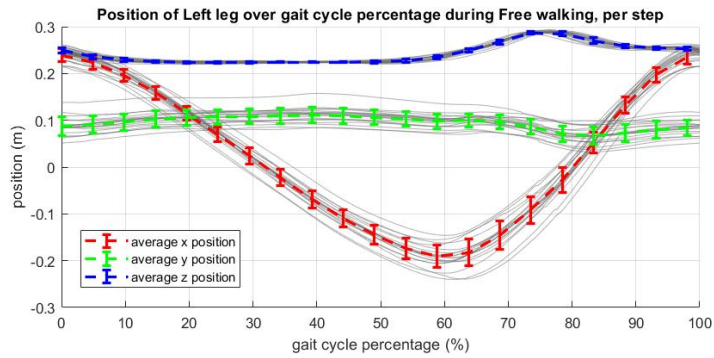


Fig. 68. Cartesian positions of the left leg motion tracker during free walking averaged over gait cycle percentage

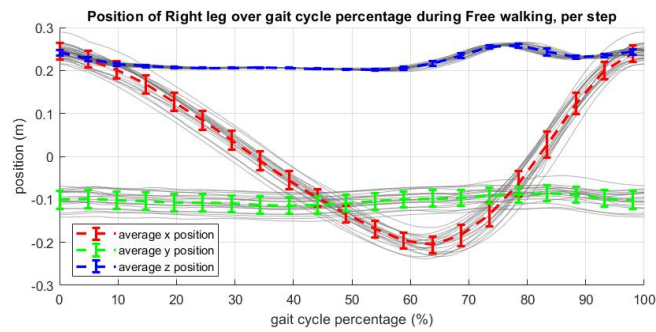


Fig. 69. Cartesian positions of the right leg motion tracker during free walking averaged over gait cycle percentage

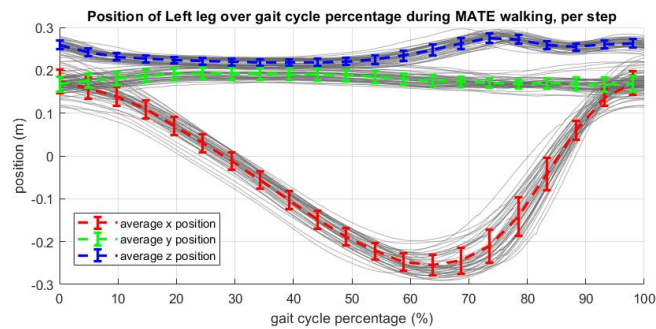


Fig. 70. Cartesian positions of the left leg motion tracker during MATE averaged over gait cycle percentage

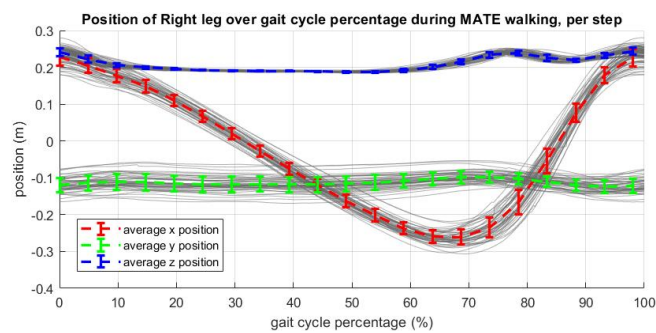


Fig. 71. Cartesian positions of the right leg motion tracker during MATE averaged over gait cycle percentage

F. Averaged Gait with Phases

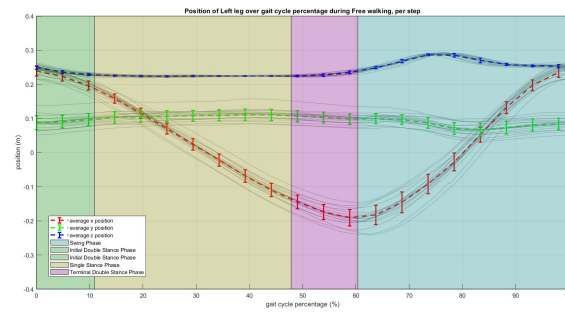


Fig. 72. Cartesian positions of the left leg motion tracker during free walking averaged over gait cycle percentage with gait phases

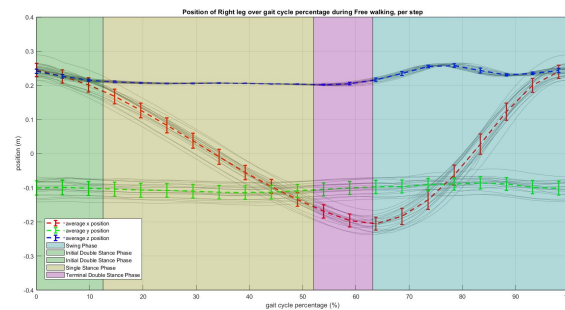


Fig. 73. Cartesian positions of the right leg motion tracker during free walking averaged over gait cycle percentage with gait phases

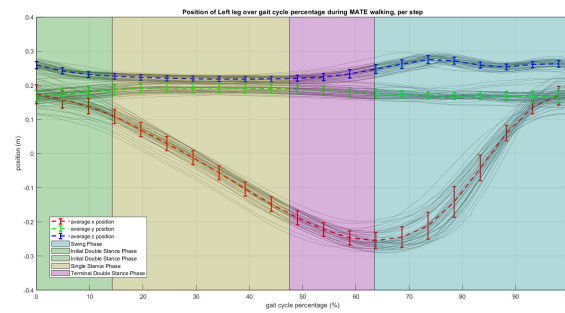


Fig. 74. Cartesian positions of the left leg motion tracker during MATE averaged over gait cycle percentage with gait phases

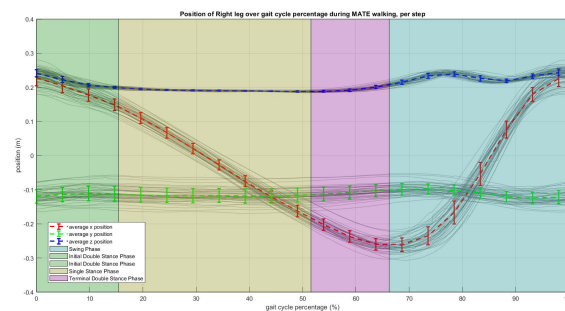


Fig. 75. Cartesian positions of the right leg motion tracker during MATE averaged over gait cycle percentage with gait phases

G. Spatio-temporal Correspondence

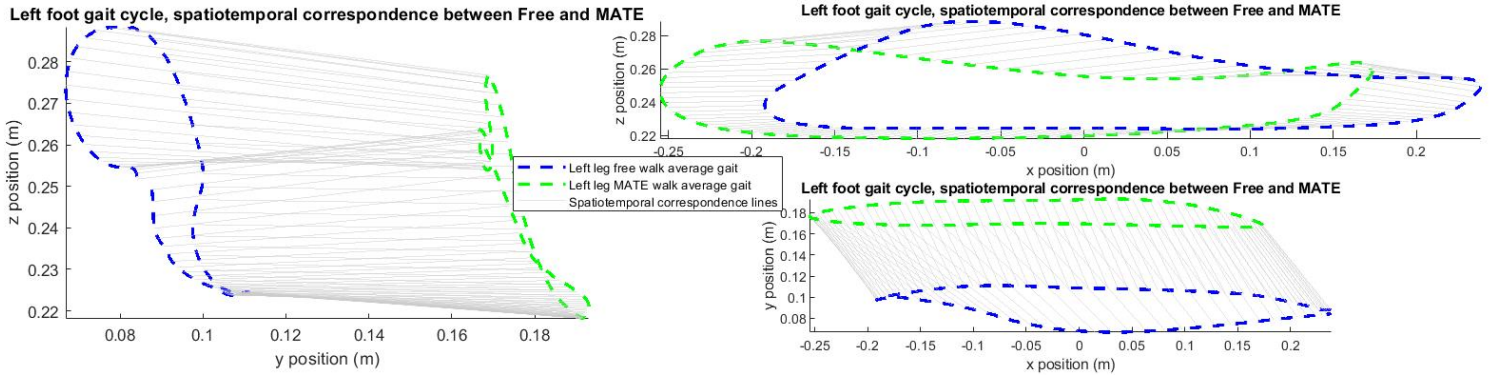


Fig. 76. Spatio-temporal correspondence between walking free and with MATE for left leg tracker, averaged gait cycle

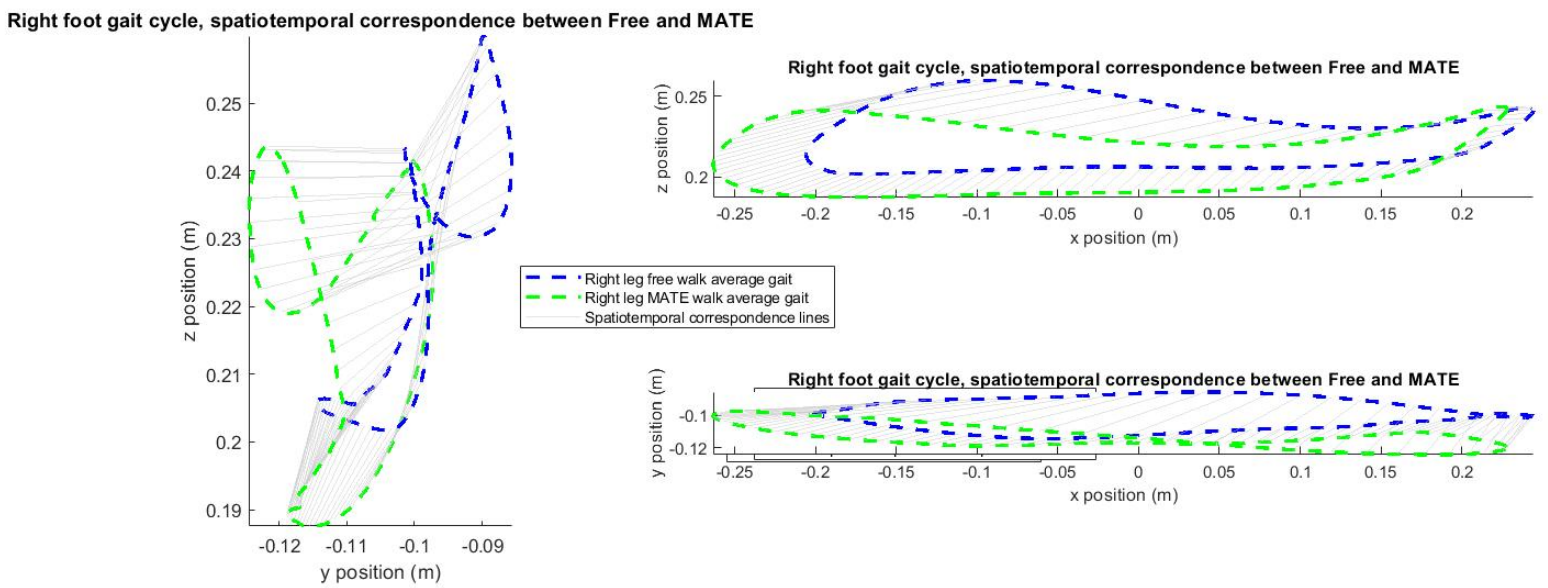


Fig. 77. Spatio-temporal correspondence between walking free and with MATE for right leg tracker, averaged gait cycle

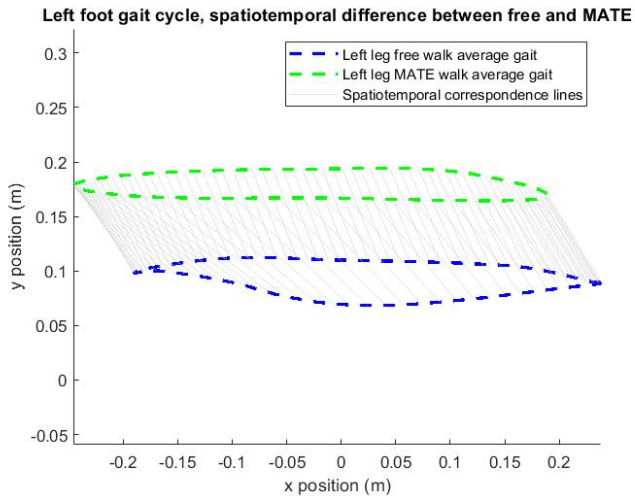


Fig. 78. Spatio-temporal correspondence between walking free and with MATE for left leg tracker, averaged gait cycle, xy

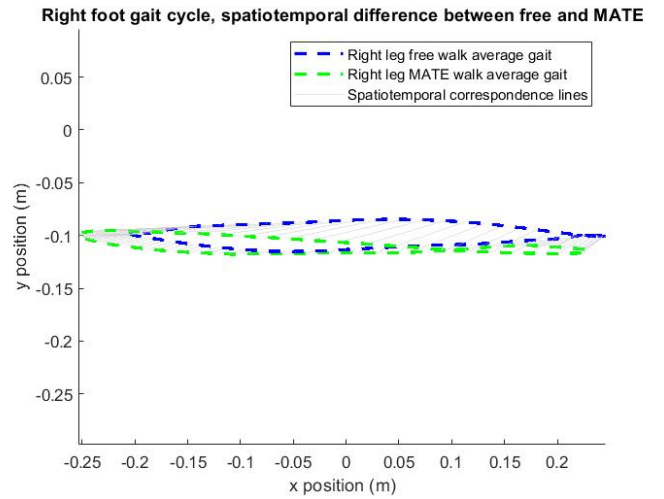


Fig. 79. Spatio-temporal correspondence between walking free and with MATE for right leg tracker, averaged gait cycle, xy

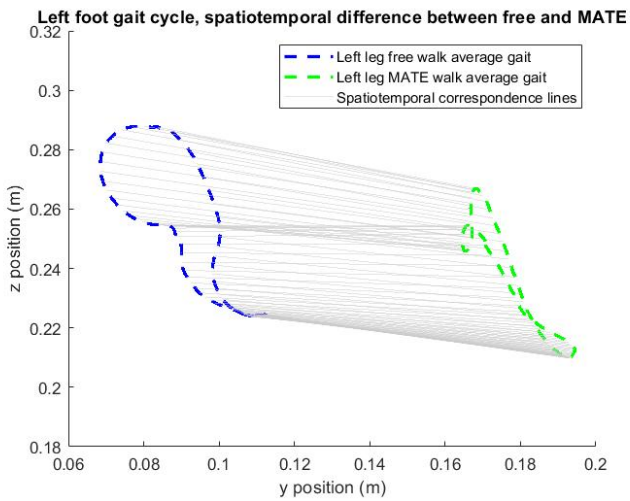


Fig. 80. Spatio-temporal correspondence between walking free and with MATE for left leg tracker, averaged gait cycle, yz

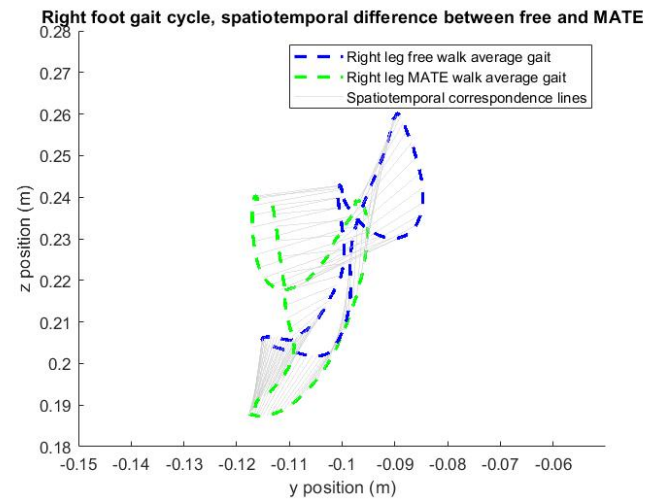


Fig. 81. Spatio-temporal correspondence between walking free and with MATE for right leg tracker, averaged gait cycle, yz

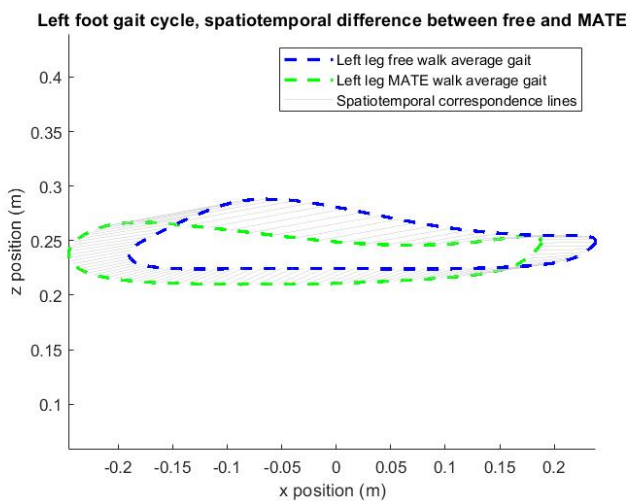


Fig. 82. Spatio-temporal correspondence between walking free and with MATE for left leg tracker, averaged gait cycle, xz

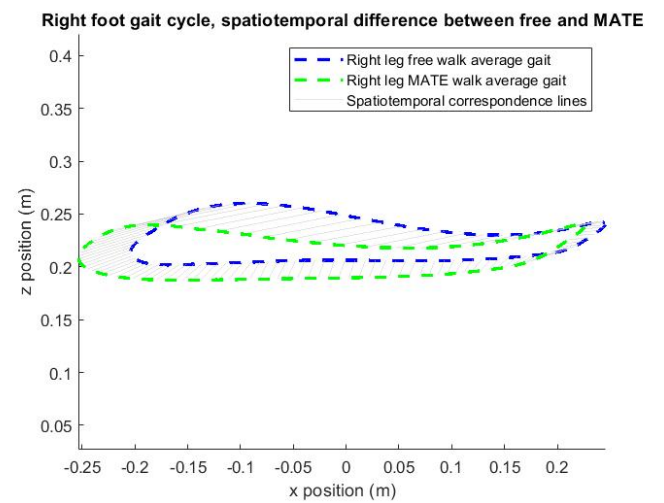


Fig. 83. Spatio-temporal correspondence between walking free and with MATE for right leg tracker, averaged gait cycle, xz

H. Forces

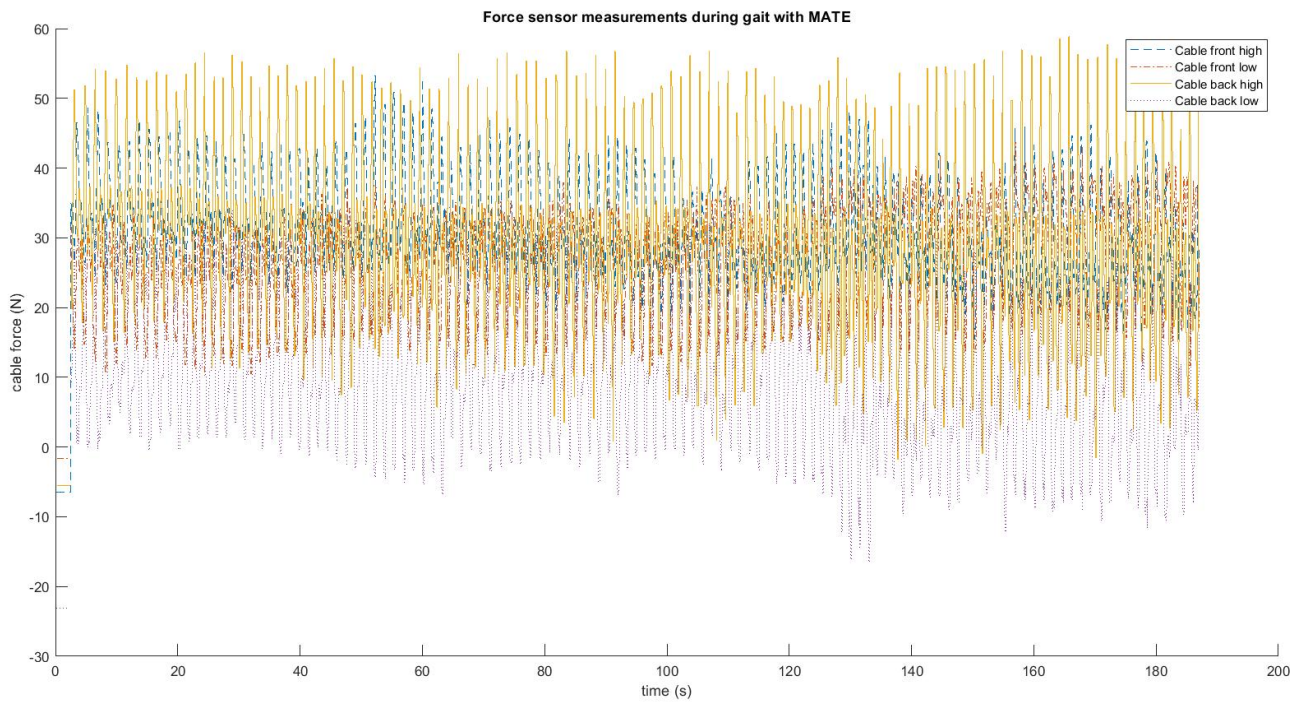


Fig. 84. Force sensor output over the entire human experiment

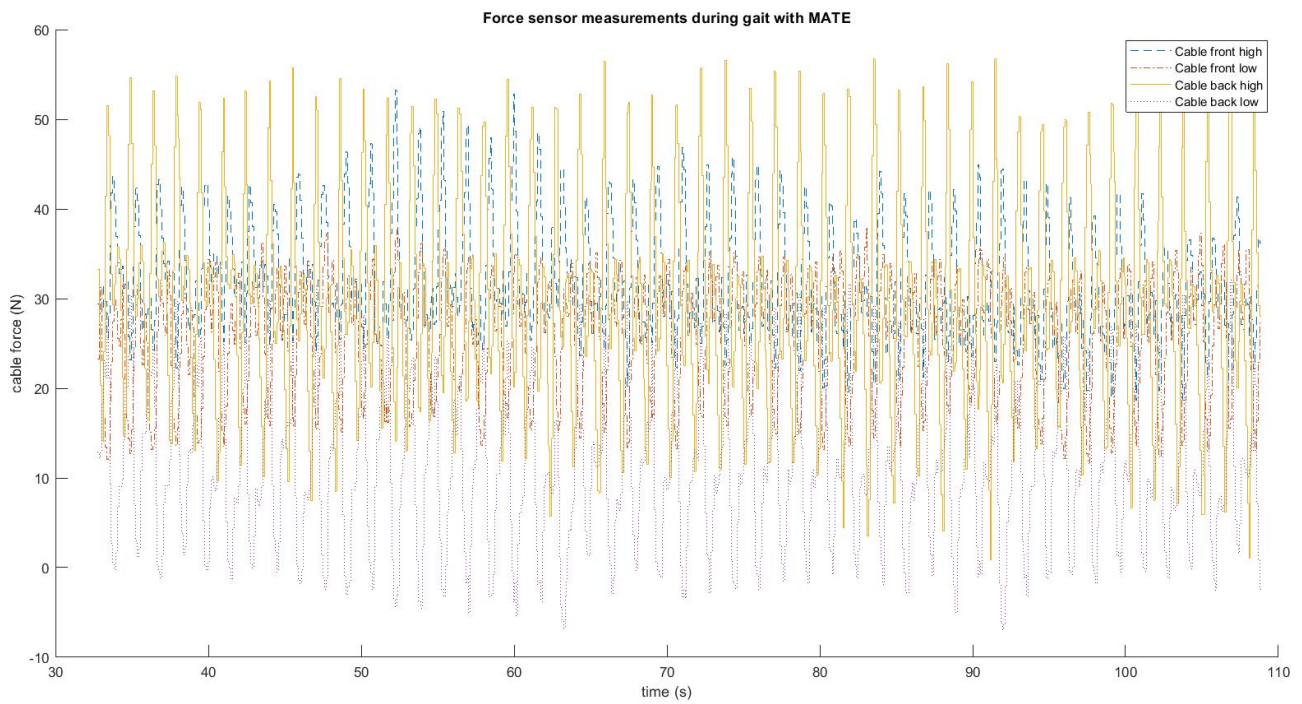


Fig. 85. Force sensor output while the participant is walking on a constant treadmill velocity

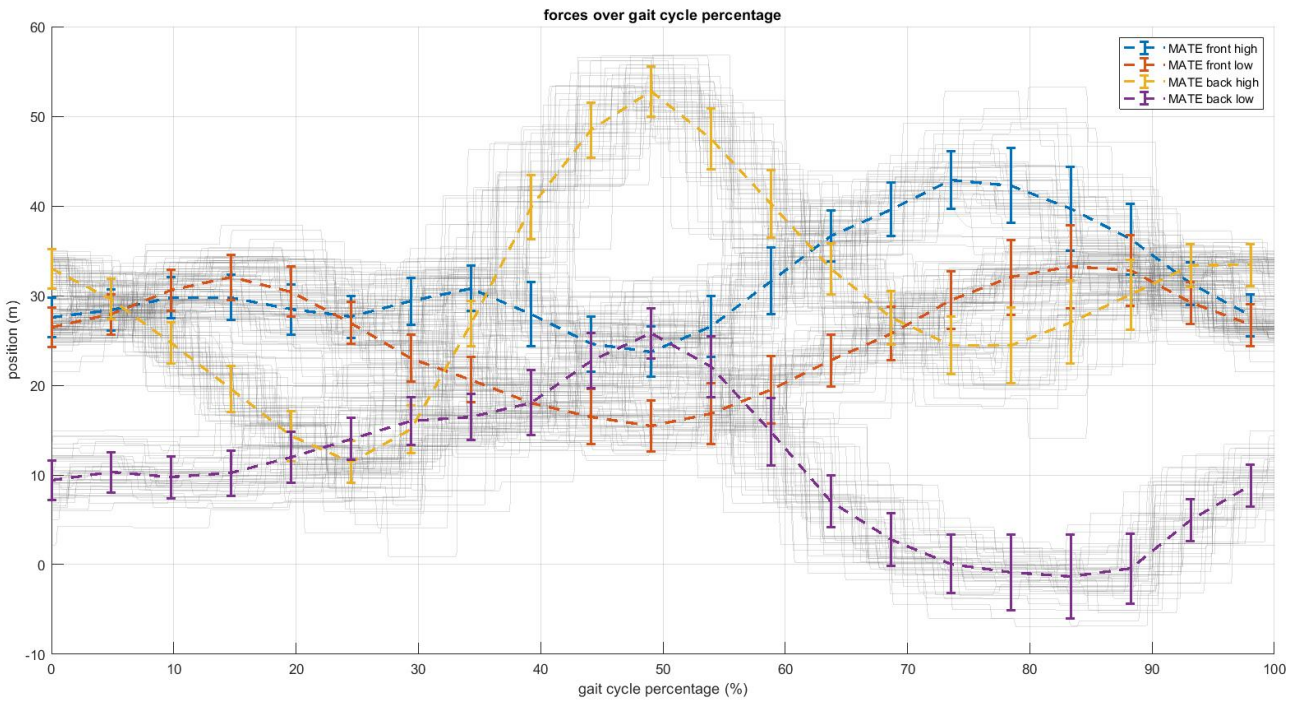


Fig. 86. Force sensor output averaged over gait cycle

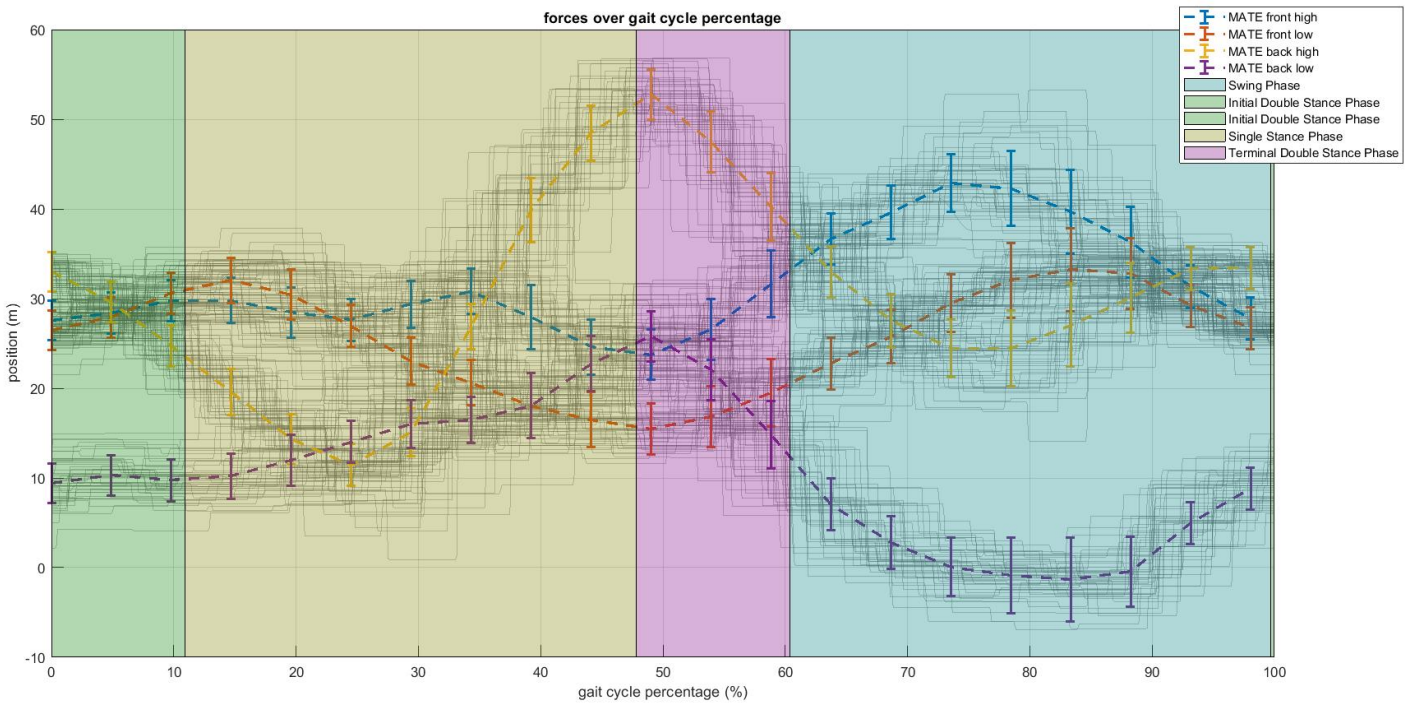


Fig. 87. Force sensor output averaged over gait cycle with gait phases

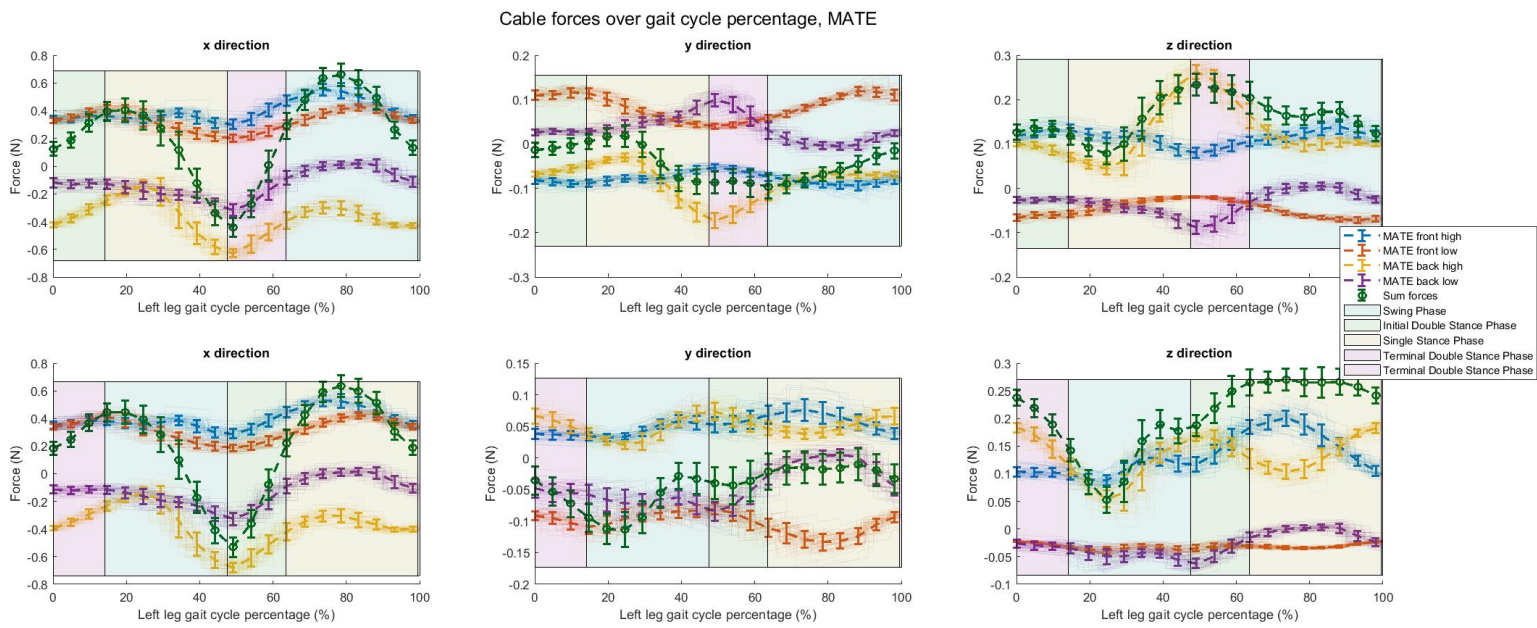


Fig. 88. Forces acting on the legs in the x and z direction, from the individual cables and their sum

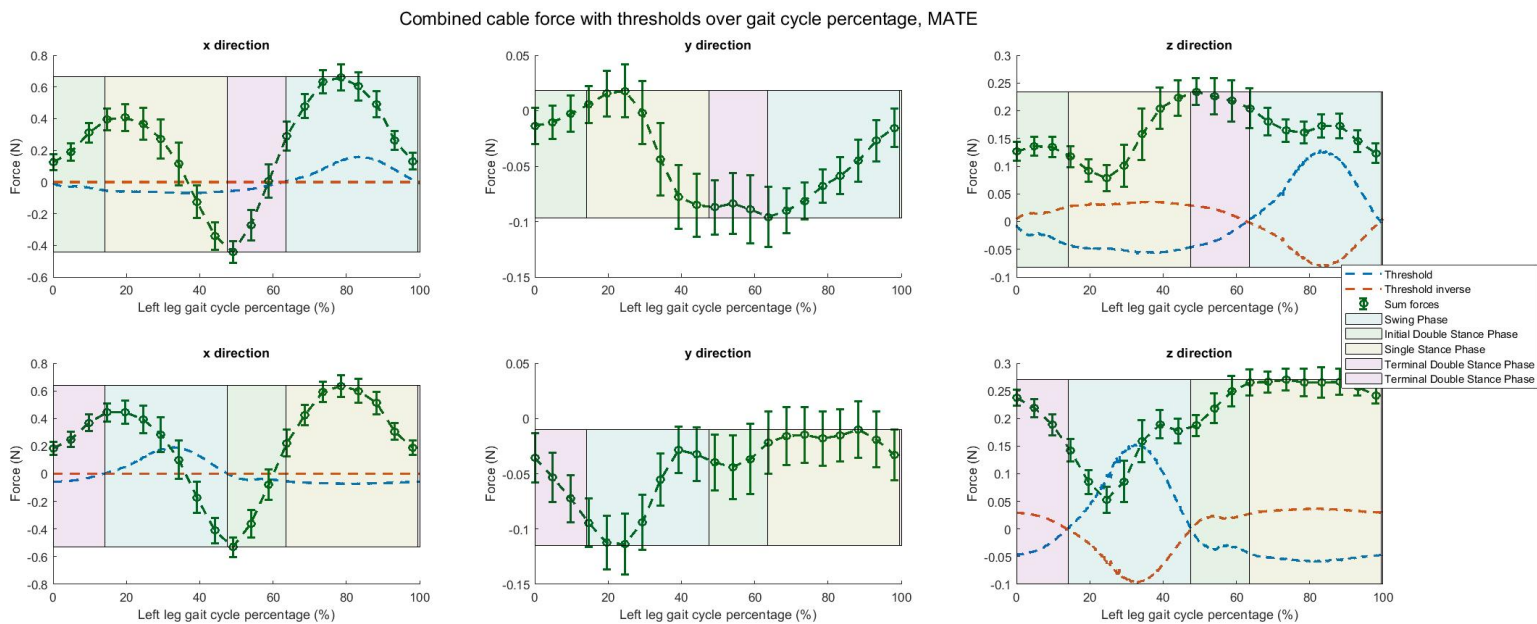


Fig. 89. Sum of cable forces compared to threshold forces as determined by [21]

APPENDIX G FORCE COMPARISON

A comparison between the measured forces and the expected forces has been performed. For a situation where the end effector positions, pulley positions and forces are known, the forces are also estimated. Using the force estimation method used in [20] with some modifications the end effector positions are transformed into forces. For this, the pretension length and non-stretch length of the cables have been estimated and a stiffness of 160 N/m is used, resulting in Figure 90. From this it can be seen that with some tuning the general shape (position of peaks and valleys) looks similar. However, the measured force

has a larger difference between the minimum and maximum force at the same elongation, indicating larger cable stiffness. For a rough estimate into the size of the forces this estimation would work. It is not accurate enough to replace measurement or to rely on for further designing purposes. Implementing more accurate measurements of the cable and accounting for non-linear stiffness might improve this estimate. Also, accounting for pulley friction is recommended, as a previous validation showed that viscous friction is non-negligible.

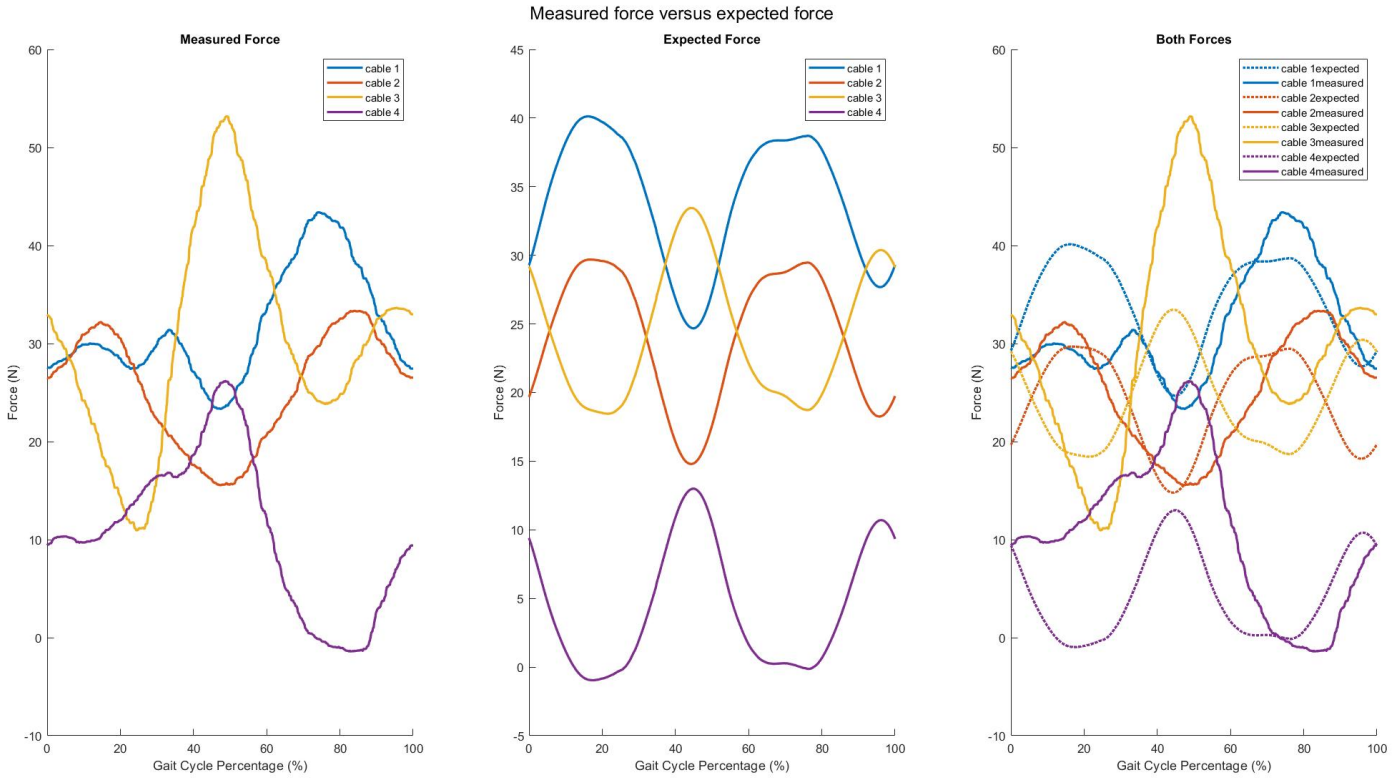


Fig. 90. Comparison between the measured force and the force as expected by [20]

APPENDIX H UNITY

A. Motion Tracking

To transform the motion capture data, a calibration procedure is followed. A box with known dimensions is placed on the global zero. A tracker is placed on the corners of the box. This means that the tracker positions in the global frame are known. At each corner the tracker is placed for 5 seconds and it is recorded in which corner the tracker is. Using a function to determine the transformation matrix, the measured tracker coordinates are transformed to what they should be in the global frame. The tracker data is transformed with this matrix, see [Figure 91](#) for the alignment. The determined transformation matrix is then applied to the rest of the recorded data, see [Figure 92](#) to see the difference between transformed and not transformed data.

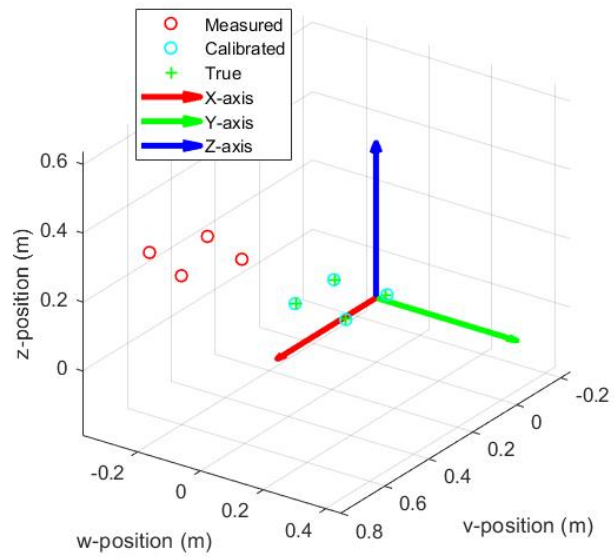


Fig. 91. Calibration of the motion capture trackers

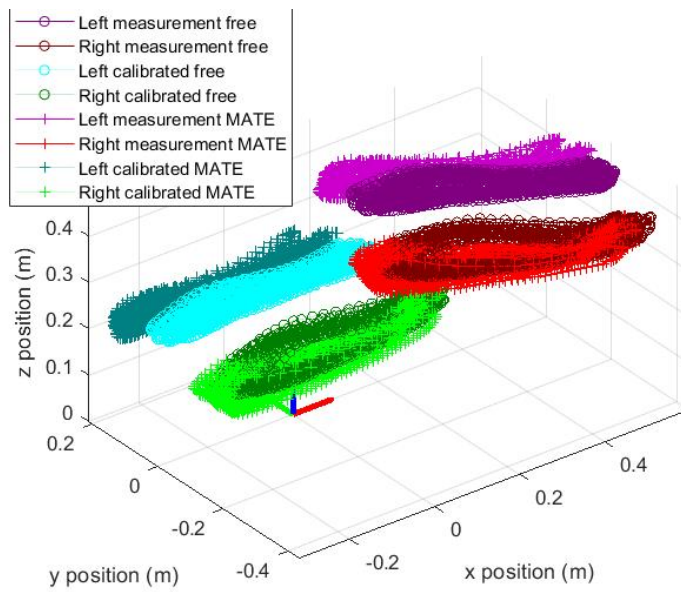


Fig. 92. Motion capture data from the left and right leg attachment points, both with and without the MATE, non-transformed and transformed